(NASA-CR-142076) THE EARTH AS A RADIO SOURCE: THE NON-THERMAL CONTINUUM Progress Report (Iowa Univ.) 54 p HC $4.25 CSCL 04A
N75-17022
Unclas
G3/46 09835

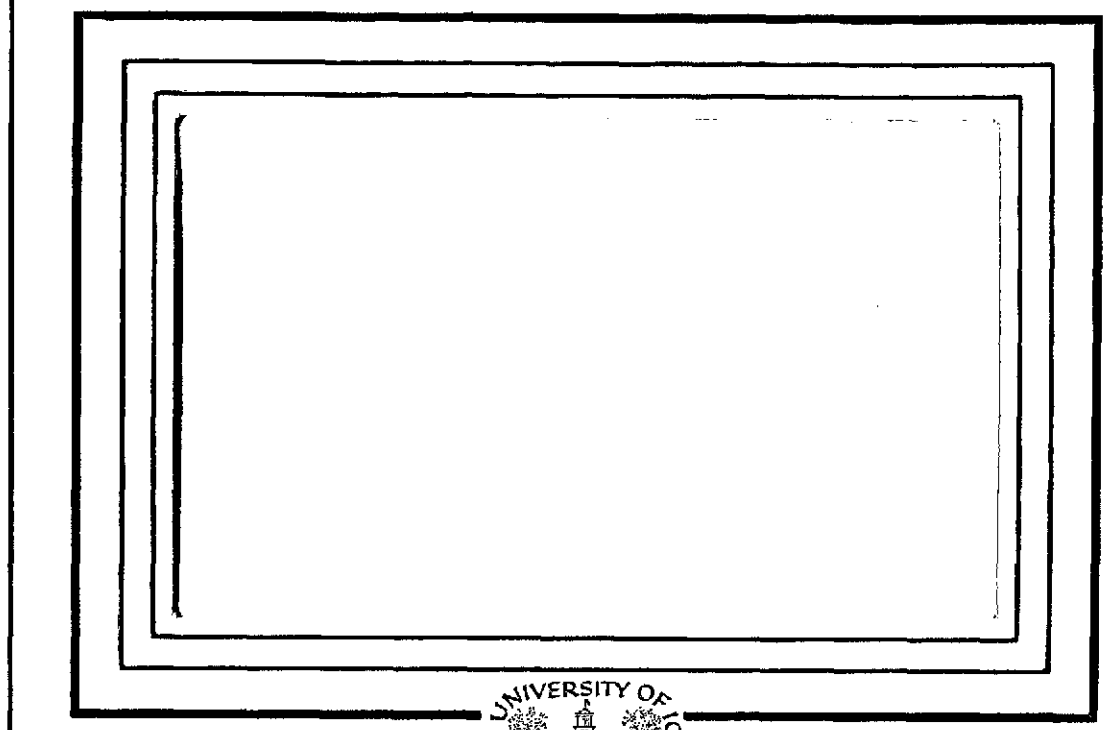

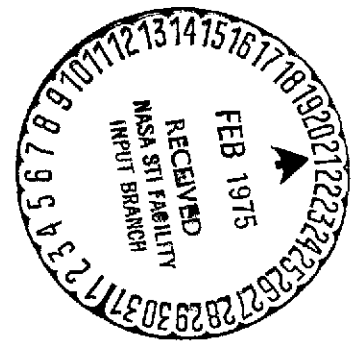

Department of Physics and Astronomy

THE UNIVERSITY OF IOWA

Iowa City, Iowa 52242

U. of Iowa/74-39

The Earth as a Radio Source: The Non-Thermal Continuum

by

Donald A. Gurnett

December, 1974

Department of Physics and Astronomy
The University of Iowa
Iowa City, Iowa 52242

This work was supported in part by the National Aeronautics and Space Administration under contracts NAS5-11074 and NAS5-11431 and Grants NGL-16-001-043 and NGL-16-001-002 and by the Office of Naval Research under Grant N00014-68-A-0196-0009.

UNCLASSIFIED

SECURITY CLASSIFICATION OF THIS PAGE (When Data Entered)

REPORT DOCUMENTATION PAGE		READ INSTRUCTIONS BEFORE COMPLETING FORM
1. REPORT NUMBER: U. of Iowa 74-39	2. GOVT ACCESSION NO.	3. RECIPIENT'S CATALOG NUMBER
4. TITLE (and Subtitle): THE EARTH AS A RADIO SOURCE: THE NON-THERMAL CONTINUUM		5. TYPE OF REPORT & PERIOD COVERED: Progress, December 1974
		6. PERFORMING ORG. REPORT NUMBER
7. AUTHOR(s): Donald A. Gurnett		8. CONTRACT OR GRANT NUMBER(s): N00014-68-A-0196-0009
9. PERFORMING ORGANIZATION NAME AND ADDRESS: Department of Physics and Astronomy, The University of Iowa, Iowa City, Iowa 52242		10. PROGRAM ELEMENT, PROJECT, TASK AREA & WORK UNIT NUMBERS
11. CONTROLLING OFFICE NAME AND ADDRESS: Office of Naval Research, Arlington, Virginia 22217		12. REPORT DATE: December 1974
		13. NUMBER OF PAGES: 52
14. MONITORING AGENCY NAME & ADDRESS (if different from Controlling Office)		15. SECURITY CLASS. (of this report): UNCLASSIFIED
		15a. DECLASSIFICATION/DOWNGRADING SCHEDULE

16. DISTRIBUTION STATEMENT (of this Report)

Approved for public release; distribution is unlimited.

17. DISTRIBUTION STATEMENT (of the abstract entered in Block 20, if different from Report)

18. SUPPLEMENTARY NOTES

To be published in J. Geophys. Res., 1975.

19. KEY WORDS (Continue on reverse side if necessary and identify by block number)

Radio Source
Non-Thermal Continuum

20. ABSTRACT (Continue on reverse side if necessary and identify by block number)

[See page following.]

DD FORM 1 JAN 73 1473 EDITION OF 1 NOV 65 IS OBSOLETE
S/N 0102-014-6601

UNCLASSIFIED

SECURITY CLASSIFICATION OF THIS PAGE (When Data Entered)

ABSTRACT

In addition to the intense and highly variable auroral kilometric radiation the earth also radiates a weak non-thermal continuum from energetic electrons in the outer radiation zone. The intensity of this continuum radiation decreases with increasing frequency and is usually below the cosmic noise level at frequencies above 100 kHz. In this paper we show that the frequency spectrum of the continuum radiation consists of two components, a trapped component, which is permanently trapped within the magnetosphere at frequencies below the solar wind plasma frequency, and an escaping component which propagates freely away from the earth at frequencies above the solar wind plasma frequency. The low frequency cutoff of the continuum radiation spectrum is at the local electron plasma frequency, which can be as low as 500 Hz in the low density regions of the distant magnetotail.

Direction finding measurements and measurements of the spatial distribution of intensity for both the trapped and freely escaping components are used to determine the region in which the continuum radiation is generated. These measurements all indicate that the continuum radiation is generated in a broad region which extends through the morning and early afternoon from about 4.0 hours to 14.0 hours local time immediately beyond the plasmapause boundary. In contrast

to the auroral kilometric radiation, which is generated in the high latitude auroral-zone regions, the continuum radiation appears to be generated over a broad range of latitudes, including the magnetic equator. In some cases the continuum radiation appears to be closely associated with intense bands of electrostatic noise which are observed near the electron plasma frequency at the plasmapause. Possible mechanisms by which this radiation could be generated, including gryo-synchrotron radiation from energetic electrons in the outer radiation zone, are discussed.

I. INTRODUCTION

Brown [1973] using radio measurements from the IMP-6 satellite has identified a weak continuum component to the radiation coming from the earth's magnetosphere in the frequency range from about 30 kHz to 110 kHz. The intensity of this continuum radiation decreases rapidly with increasing frequency, varying approximately as $f^{-2.8}$ (f = frequency), and is usually below the cosmic noise level at frequencies above about 100 kHz. The low frequency limit at about 30 kHz is apparently caused by the propagation cutoff at the local plasma frequency in the solar wind. Frankel [1973] has also studied this radiation and concludes that the noise is produced by gyro-synchrotron radiation from energetic electrons in the outer radiation zone.

Gurnett and Shaw [1973] have also identified another somewhat more intense continuum component at even lower frequencies, from about 5 kHz to 20 kHz. This continuum radiation occurs at frequencies below the solar wind plasma frequency and is permanently trapped within the low density regions of the magnetospheric cavity. The purpose of this paper is to investigate the basic features of the non-thermal continuum radiation from the earth's magnetosphere using radio and plasma wave measurements from the IMP-6 and IMP-8 satellites. We show that the continuum radiation reported by Brown [1973] and the

trapped radiation reported by Gurnett and Shaw [1973] are simply different portions of a single non-thermal continuum spectrum which extends from frequencies as low as 500 Hz to greater than 100 kHz. Direction finding measurements and spatial surveys of the intensity of this radiation are used to determine the region of the magnetosphere in which the noise is generated.

The data analyzed in this study are obtained from the University of Iowa plasma wave experiments on the IMP-6 and IMP-8 satellites. The IMP-6 spacecraft is in a highly eccentric orbit with initial perigee and apogee geocentric radial distances of 1.04 R_e and 33.0 R_e, respectively, orbit inclination of 28.7 degrees, and period of 4.18 days. The IMP-8 spacecraft is in a low eccentricity orbit with initial perigee and apogee geocentric radial distances of 23.1 R_e and 46.3 R_e, respectively, orbit inclination of 28.6 degrees, and period 11.98 days. The IMP-6 measurements are particularly useful for studying the radial dependence of terrestrial radio emissions over a very wide range of radial distances, whereas the IMP-8 measurements are particularly useful for obtaining a rapid survey of all local times at a roughly constant radial distance.

The plasma wave experiments on both spacecrafts are designed to make measurements over a very broad frequency range, 20 Hz to 200 kHz for IMP-6, and 40 Hz to 2.0 MHz for IMP-8. Both experiments use "long" electric dipole antennas, 92.5 meters tip-to-tip for IMP-6 and 121.5 meters tip-to-tip for IMP-8, which are extended outward perpendicular to the spacecraft spin axis. The spin axes of both

spacecrafts are oriented very nearly perpendicular to the ecliptic plane. Further technical details of these experiments are given by Gurnett and Shaw [1973] and Gurnett [1974].

II. CHARACTERISTICS OF THE NON-THERMAL CONTINUUM

The term continuum, as used in this paper, refers to radiation which has a smooth monotonic frequency spectrum extending over a frequency range of several octaves with an essentially constant intensity on a time scale of a few hours or less. Non-thermal continuum radiation from the earth's magnetosphere is difficult to detect because the radiation is very weak, only slightly above the noise level of the IMP-6 and IMP-8 plasma wave experiments, and is often masked by other intense radio and plasma wave emissions which occur in the same frequency range. Auroral kilometric radiation [Gurnett, 1974], which occurs in the frequency range from about 50 kHz to 500 kHz, often has intensities 60 db to 80 db above the level of the quiescent continuum. Electrostatic plasma wave turbulence in the magnetosheath and bow shock, electron plasma oscillations in the solar wind, and type III radio noise bursts also frequently interfere with measurements of the continuum radiation. Measurements of the non-thermal continuum radiation from the earth's magnetosphere must, therefore, be carefully selected to avoid contamination from other sources.

A typical IMP-8 measurement of the continuum radiation is illustrated in Figure 1. The outputs from 16 channels of the electric field spectrum analyzer are shown for a 24 hour period in which the spacecraft is located in the solar wind at a geocentric radial

distance of about 42.0 R_e and a local time of about 17.5 hours. The ordinate for each frequency channel is proportional to the logarithm of the electric field amplitude in that frequency channel. The interval from the baseline of one channel to the baseline of the next higher channel represents a dynamic range of 100 db. The vertical bars, which make up the black portion of each plot, indicate the amplitude averaged over a time interval of 163.48 seconds and the dots indicate the maximum amplitude over the same time interval. Throughout this 24 hour period many intense bursts of auroral kilometric radiation are evident in the higher frequency channels. Only one brief period, from about 1005 UT to 1115 UT, occurs during which the intensity of the auroral kilometric radiation is sufficiently low to permit an accurate measurement of the spectrum of the quiescent continuum radiation. During this period the average noise level in all channels is essentially constant. The noise levels in the 22.0 kHz to 178.0 kHz channels are, however, slightly above the receiver noise level. Spin modulation measurements during this period show that the radiation detected in these channels is coming from the vicinity of the earth. The frequency spectrum of this radiation has a distinct peak in the 22.0 kHz channel and decreases in intensity at higher frequencies. No radiation is detectable coming from the direction of the earth above 178.0 kHz or below 22.0 kHz. The relatively high constant noise level evident in the 2.0 MHz channel is the galactic background.

Another example in which the spectrum of the non-thermal continuum is clearly evident in the IMP-8 data is illustrated in

Figure 2. In this case the spacecraft is in the distant magnetotail at a geocentric radial distance of about 41.0 R_e and a local time of about 23.5 hours. At high frequencies the spectrum of the continuum radiation is qualitatively similar to the spectrum observed in the solar wind, however in this case the radiation extends down to a frequency of about 5.60 kHz which is considerably below the cutoff frequency observed in the solar wind. At the lower frequencies, where no auroral kilometric radiation is present, it is evident that the continuum radiation exists with an essentially constant amplitude throughout the magnetotail. In some cases, such as at about 1400 UT, the spectrum of the continuum radiation extends down to frequencies as low as 562 Hz.

To illustrate the general character of the continuum spectrum at different points around the earth Figure 3 shows five spectrums selected at various representative local times. Four of these spectrums were obtained in the solar wind and one, in the center panel, was obtained in the distant magnetotail. The spectrums in the solar wind all show the same basic characteristics, consisting of a monotonic decrease in intensity with increasing frequency and a sharp cutoff near the solar wind plasma frequency, at about 20 kHz to 30 kHz. These spectrums are in good qualitative and quantitative agreement with the continuum radiation spectrums reported by Brown [1973] and Frankel [1973]. The spectrum in the magnetotail shows the same basic characteristics as the trapped electromagnetic radiation described by Gurnett and Shaw [1973], consisting of a flat peak extending from about

5 kHz to 20 kHz, a sharp low frequency cutoff at the local electron plasma frequency, and a rapidly decreasing intensity above 20 kHz. In comparing the continuum radiation spectrums obtained in the solar wind and in the magnetotail it is evident that the spectrums are nearly identical at all frequencies above the propagation cutoff at the solar wind plasma frequency. This similarity strongly suggests that the noise in both regions comes from the same source and that the spectrum observed in the solar wind represents that portion of the continuum radiation which can escape into the solar wind above the solar wind plasma frequency.

The relationship between these various spectrums is summarized in Figure 4, which shows representative spectrums for the galactic continuum, the very intense and highly variable auroral kilometric radiation, and the relatively steady non-thermal continuum radiation. The spectrum of the continuum radiation can be divided into two components, a trapped component, which is permanently trapped within the magnetospheric cavity at frequencies below the solar wind plasma frequency, and an escaping component, which can propagate freely away from the earth at frequencies above the solar wind plasma frequency. This cateogrization of the various radio emission spectrums of the earth should not be regarded final since it is virtually certain that other weak, but possibly significant, components may also exist. For example, a small but distinct peak is evident at about 178 kHz in all the spectrums shown in Figure 3. It is not known whether this peak is associated with a distinctly different source, as suggested by Kaizer and Stone [1974], or simply represents a quiescent level of the auroral kilometric radiation.

III. THE TRAPPED COMPONENT

A. Direction Finding Measurements

The distinction between the trapped and free escape components of the non-thermal continuum is particularly evident in the direction finding measurements of this radiation. Since the spin axes of both IMP-6 and IMP-8 are perpendicular to the ecliptic plane, with the electric dipole antenna axis perpendicular to the spin axis, the position of a radio source in the ecliptic plane can be determined from the spin modulation of the observed signal strength. The null direction, δ, and modulation factor, m, are determined by fitting the equation

$$\left(\frac{E}{E_o}\right)^2 = \left(1 - \frac{m}{2}\right) - \frac{m}{2} \cos\left[2(\delta_y - \delta)\right] \qquad (1)$$

to the normalized field strength, E/E_o. The angle, δ_y, is the azimuthal orientation of the antenna with respect to the satellite-earth line. The detailed procedures used to compute the best fit values for δ and m are discussed by Kurth et al. [1975].

A typical set of direction finding measurements obtained by IMP-8 in the distant magnetotail are shown in Figures 5 and 6. In each case the trapped continuum radiation is evident at low frequencies, less than about 50 kHz, and auroral kilometric radiation is evident

at high frequencies, greater than 50 kHz. The null direction, δ, measured positive eastward with respect to the spacecraft-earth line, is shown as a function of frequency in the bottom panel of each figure. At high frequencies, above about 30 kHz, the null directions of both the continuum radiation and the auroral kilometric radiation is within few degrees of the direction to the earth. At frequencies below about 30 kHz a distinct shift in the null direction away from the earth is evident. In both cases, one in the late evening (LT = 22.5 Hr.) and the other in the early morning (LT = 1.8 Hr.), the null direction shifts toward the sun at frequencies below about 30 kHz. A corresponding decrease in the modulation factor also occurs at this frequency, from $m \simeq 0.8$ at frequencies above 30 kHz to $m \simeq 0.2$ at frequencies below 30 kHz. The frequency at which this transition occurs corresponds closely with the solar wind plasma frequency as indicated by the vertical dashed line labeled "f_p solar wind" in Figures 5 and 6. The solar wind plasma frequency measurements were obtained from the Los Alamos solar wind plasma experiment on the IMP-7 spacecraft [personal communication, M. Montgomery, 1974]. IMP-7 was located in the solar wind upstream from the earth at the time that the measurements in Figures 5 and 6 were made. The shifts in the null direction and modulation factor at approximately the solar wind plasma frequency evidently correspond to the transition from the free escape to the trapped regimes illustrated in Figure 4. The tendency for the null direction of the trapped continuum radiation to lie along the earth-sun line is a general characteristic of all the IMP-8 direction

finding measurements in the distant magnetotail. This dependence is illustrated in Figure 7 which shows a series of null direction measurements made at 16.5 kHz during three IMP-8 passes through the distant magnetotail. The null direction is seen to closely follow the sun direction, except for a slight deviation toward the earth near the magnetopause boundaries, which occur at about $\phi_{GSE} = 140°$ and $220°$ during these passes.

The shift in the null direction near the solar wind plasma frequency and the tendency for the null direction of the trapped continuum radiation to be aligned along the earth-sun line can be explained from simple propagation considerations. Since radiation at frequencies below the magnetosheath plasma frequency is reflected at the magnetopause the surface of the magnetopause apparently acts as a large parabolic reflector, directing radiation from near the earth into the magnetotail as illustrated in Figure 8. Because the direction finding measurement responds to the average source position the null direction tends to be aligned along the earth-sun line in the distant magnetotail. There is, of course, the question to what extent the magnetospheric cavity acts as a perfectly lossless cavity. If the cavity has an extremely high "Q" then the radiation would be expected to be isotropic since multiple reflections would rapidly randomize the radiation and no spin modulation would be evident. Since a significant and easily detectable level of spin modulation ($m \simeq 0.2$) does exist it is concluded that a sizable flux of radiation is lost into the downstream tail region, resulting in a relatively low

Q for the cavity. Further evidence that the Q of the cavity is quite small is given by the fact that the intensity of the continuum radiation increases only slightly (possibly a factor of two) as the frequency changes from the free escape to the trapped regime. Thus, there is relatively little build up of the radiation intensity within the cavity due to multiple reflections. Note that the transition from the trapped to free escape regime is actually not an abrupt transition since the magnetosheath plasma frequency varies from approximately the solar wind value in the downstream region to approximately twice this value at the stagnation point. Also, some reflection or scattering of the incident radiation may occur in the magnetosheath, even at frequencies above the local plasma frequency.

B. Spatial Distribution of Intensity

To understand the origin of continuum radiation we must first establish the region in which the noise is generated. Unfortunately, for the trapped component, direction finding measurements do not provide much useful information on the source location because of the complicated reflections which occur at the magnetopause. We have therefore investigated the spatial distribution of the intensity of the trapped continuum to try to determine the source region. Because the intensity of the trapped continuum radiation undergoes long term temporal fluctuations on the order of 10 db [see Gurnett and Shaw, 1973] a large number of measurements must be used to obtain a reliable spatial distribution. Three years of IMP-6 data, totaling about 800,000 intensity measurements (163.48 second averages), are used in

this study. Since it is impossible to manually identify the continuum radiation for such a large number of measurements a criterion was devised to provide computer identification of the trapped continuum radiation. The criterion used is to require that the ratio of the peak to average field strength in each 163.48 second period not exceed 1.2 and that the average difference between adjacent peak field strength not exceed 1 db. This criterion eliminates impulsive noise bursts such as whistlers, chorus, and magnetosheath electrostatic turbulence. The criterion was tested manually on several orbits and has been verified to provide correct identification of the trapped continuum radiation with a very high degree of confidence. The 16.5 kHz channel was chosen as representative of the trapped continuum radiation. This frequency was chosen because it is almost always below the solar wind plasma frequency and yet above the local plasma frequency inside the magnetospheric cavity. The measured intensities in this channel were average in blocks defined by 16 radial distance intervals from 1.0 R_e to 39.8 R_e and 12 local time intervals from 0.0 Hr. to 24.0 Hr. The results of this averaging procedure are shown in Figure 9.

The intensity of the continuum radiation at 16.5 kHz is seen to be remarkably constant at a level of about 0.5 to 1.0 times 10^{-18} watt m^{-2} Hz^{-1}. As expected, a sharp cutoff is evident at radial distances corresponding to the magnetopause and plasmapause boundaries. Although the intensity is constant over a large region of the magnetosphere a distinct maximum, considerably above the statistical uncertainty in

the average computation and approximately a factor of two above the overall average, occurs in the local time range from 4.0 hours to 14.0 hours and in the radial distance range from 5.01 R_e to 7.94 R_e. The existence of this maximum can also be verified by direct comparison of individual passes through this region with passes through other regions of the magnetosphere. Although the interpretation of this intensity distribution is greatly complicated by the many reflections and complicated ray paths which can occur within the magnetospheric cavity (thereby accounting for the nearly uniform intensity distribution) the existence of a distinct region of maximum intensity strongly suggests that a major fraction of the trapped continuum radiation is generated within this region.

IV. THE ESCAPING COMPONENT

A. Direction Finding Measurements

Direction finding measurements of the escaping continuum radiation provide a much better method of determining the source region of the continuum radiation since this radiation propagates directly to the spacecraft without reflection at the magnetopause. The 56.2 kHz frequency channel has been chosen to perform direction finding measurements of the escaping continuum radiation. This frequency is chosen because it is usually below the frequency range of the intense auroral kilometric radiation, which often masks the weak continuum radiation, and yet well above the plasma frequency normally encountered in the magnetosheath and solar wind.

A total of 184 intervals, each from 1 to 4 hours in duration have been selected from the first 18 orbits of IMP-8 to study the direction of propagation of the escaping continuum radiation at 56.2 kHz. These intervals are all selected such that no radiation other than the continuum is detectable. For each interval the best fit null direction δ and modulation factor m are computed and the r.m.s. error in the fit of Equation 1 to the measured field strengths is determined. From these quantities the distance of closest approach of the ray path to the earth, $\rho_\perp$, projected into the ecliptic plane, and the r.m.s. uncertainty, $\sigma_{\rho\perp}$, in $\rho_\perp$ are computed. Because the

power flux is sometimes too small to provide reliable direction finding measurements only those cases for which the uncertainty in $\rho_\perp$ is less than 2 R_e ($\sigma_{\rho\perp} \leq 2\ R_e$) are used in this study. Of the 184 cases selected 82 satisfied this error criterion. The threshold power flux for providing reliable direction finding measurements ($\sigma_{\rho\perp} \leq 2\ R_e$) at 56.2 kHz is about 5×10^{-21} watts m^{-2} Hz^{-1}. The median power flux of the 82 cases selected for this study is about 1.0×10^{-20} watts m^{-2} Hz^{-1}, and the maximum power flux observed is 2×10^{-19} watts m^{-2} Hz^{-1}.

The distribution of transverse source positions determined for these 82 cases is shown in Figure 10. Most of the direction finding measurements show an apparent source position well inside the magnetosphere, with transverse source positions typically less than 8 R_e. However, a few cases are observed with source positions as much as 20 R_e from the earth. For the present we consider only those cases for which the source appears to be definitely within the magnetosphere, specifically those with $|\rho_\perp| \leq 8\ R_e$. The anomalous cases with $|\rho_\perp| > 8\ R_e$ are discussed later.

The ray paths for the cases with $|\rho_\perp| \leq 8\ R_e$ are shown in Figure 11, projected into the ecliptic plane. The spacecraft position for each ray path is shown as a dot and the arrow indicates the direction of the null. The apparent center of the source region can be estimated from the intersection of ray paths observed at various local times. It is evident that most of the ray paths tend to intersect on the local morning and local day side of the earth at a radial distance, projected into the ecliptic plane, of about 2 R_e to 3 R_e

from the center of the earth. It is also evident that a great deal of scatter exists in the apparent source position, indicative of a broad and somewhat variable source region.

A quantitative estimate of the angular size of the source can be obtained from the modulation factor, m. If the source is located in the plane of rotation of the antenna a very small (point) source produces a very deep null ($m \simeq 1$), whereas a very broad source produces very little modulation ($m \simeq 0$). In practice, quantitative estimates of the source size are complicated by the fact that the source is seldom exactly in the plane of rotation of the antenna (this occurs only when the geocentric solar ecliptic latitude of IMP-8 is zero, $\lambda_{GSE} = 0°$, which happens only twice per orbit). Also the receiver noise level tends to decrease the modulation factor, particularly at low signal to noise ratios. Figure 12 shows the distribution of modulation factors for continuum radiation at 56.2 kHz measured at times when the earth is within $\pm$ 20° of the plane of rotation of the electric antenna ($|\lambda_{GSE}| \leq 20°$). The modulation factor, M, used in this figure has been corrected for the effects of the receiver noise level, and also for the first order effect caused by the deviation of the source location (assumed to be at the center of the earth) out of the plane of rotation of the electric antenna. This correction is made by dividing the measured modulation index by $\mathrm{Cos}^2 \lambda_{GSE}$,

$$M = m/\mathrm{Cos}^2 \lambda_{GSE},$$

which is the expected variation for a small source located at the center of the earth. The geocentric solar ecliptic latitude, λ_{GSE}, has been limited to $\pm$ 20° to limit the size of the $Cos^2 \lambda_{GSE}$ correction, as well as other errors, such as polarization dependencies, which affect the modulation factor.

From Figure 12 it is seen that the corrected modulation factor for the continuum radiation is typically about 0.8 to 0.9. A rough indication of the source size is given at the top of Figure 12, based on two point sources located in the ecliptic plane on opposite sides of the earth. These data indicate that the source subtends a very large half angle of about 20° as viewed from IMP-8 at radial distances (projected into the ecliptic plane) of about 20.0 R_e to 30.0 R_e. Because of the aforementioned corrections which must be performed to obtain the modulation factor these quantitative determinations of the source size must be considered somewhat uncertain, particularly when the continuum radiation is very weak. The actual source size is probably somewhat smaller than indicated by Figure 12 since most of the errors introduced tend to decrease the modulation factor, hence increase the apparent source size. It is clear, however, that the source of the continuum radiation is much larger than a source of the auroral kilometric radiation, which typically has a modulation factor of 0.95 to 0.98.

B. Spatial Distribution of Intensity

Further information on the source region of the escaping continuum radiation can be obtained from the spatial distribution of

intensity. Since the escaping continuum radiation is not reflected by the magnetopause the region of maximum intensity should provide a good indication of the source region. Data from the IMP-6 spacecraft, which has a highly eccentric orbit, must be used to provide measurements in the source region. Unfortunately the IMP-6 experiment is about a factor of 5 less sensitive than the IMP-8 experiment, so the continuum radiation generally cannot be detected by IMP-6 at large radial distances or when the radiation is very weak. The noise level of the IMP-6 experiment is about 2.5×10^{-20} watts m^{-2} Hz^{-1} at 56.2 kHz. Since the intensity of the continuum radiation does vary considerably many periods do however exist when the continuum radiation is sufficiently intense to provide good measurements of the spatial distribution with the IMP-6 experiment.

Three cases in which the continuum radiation at 56.2 kHz is sufficiently intense to clearly show the radial variation of the intensity are shown in Figure 13. In each case the spacecraft is moving outward to larger radial distances, from about 3.0 R_e to 8.0 R_e, in the local morning region of the magnetosphere. The plasmapause location is identified on each plot as the point where the local plasma frequency, f_p, is approximately equal to 56.2 kHz. The plasma frequency is obtained from the upper hybrid resonance noise band which occurs immediately following the arrow marked $f \simeq f_p$ in each plot (see Shaw and Gurnett [1975] for a discussion of the upper hybrid resonance noise). No continuum radiation whatever is detectable inside of the plasmapause. Outside of the plasmapause, where $f > f_p$, moderately

intense continuum radiation is evident in each case. In the top two examples, the maximum intensity of the continuum radiation occurs at the point where the intense upper hybrid noise band occurs. In the bottom example, the maximum intensity occurs well beyond the plasmapause, at a radial distance of about 5.0 R_e.

To provide a quantitative determination of the region of maximum intensity for the escaping continuum radiation the average power flux has also been computed as a function of local time and radial distance at 56.2 kHz using three years of IMP-6 data. To assure that only continuum radiation is included in this average only measurements which fluctuate by less than 1 db in any 163.48 second interval and which have a ratio of peak to average field strength less than 1.4 are used. The average field strengths obtained, using this selection criterion for the 56.2 kHz channel, are shown in Figure 14. Although considerable scatter is evident in the radial distribution at low intensities a very distinct maximum is evident in the average power flux at radial distances from about 3.98 R_e to 7.94 R_e and in the local time range from about 4.0 hours to 14.0 hours local time. The average power flux in this region, $> 5.0 \times 10^{-20}$ watts m^{-2} Hz^{-1}, is well above the receiver noise level.

The region of maximum intensity for the escaping continuum radiation shown in Figure 14 agrees well with the source region indicated by the direction finding measurements in Figure 11 and is also consistent with the region of maximum intensity found for the trapped continuum radiation. Based on these results it is concluded that the

source region of the continuum radiation is located in a broad region beyond the plasmapause boundary (where $f \simeq f_p$) in the morning and early afternoon at local times from about 4.0 hours to 14.0 hours. Since the continuum radiation is often observed immediately beyond the plasmapause near the magnetic equator, as in the top two examples of Figure 13, it is also concluded that the continuum radiation is generated near the magnetic equator and is not a high latitude auroral-zone emission. A qualitative illustration of the generation region suggested by these results is shown in Figure 15. The propagation cutoff surface at $f \simeq f_p$ tends to follow the shape of the plasmapause because of the rapid change in the electron density near this boundary. The distinct outward bulge in the plasmasphere in the local evening is a well known feature of the plasmapause [Carpenter, 1970].

V. RADIATION ASSOCIATED WITH THE BOW SHOCK AND/OR MAGNETOSHEATH

As shown in Figure 10 and discussed earlier a small but distinct fraction of the direction finding measurements at 56.2 kHz indicate source locations well outside of the magnetosphere, with transverse source positions greater than 8 R_e, and sometimes as large as 20 R_e. These apparently anomalous cases have been carefully examined to make certain that the direction finding measurements are not being influenced by some spurious effect such as telemetry errors or interference from solar radio noise bursts. No such effect could be found. In many of these cases the computed uncertainty in the null direction is very small, less than 1°, indicating that a very reliabile fit was obtained to the observed spin modulation.

Figure 16 shows the ray path directions, projected into the ecliptic plane, for the anomalous direction finding measurements at 56.2 kHz. The most strking feature of this plot is that most of the ray paths appear to come from the general region of the bow shock and/or magnetosheath, particularly from the morning side of the magnetosphere. Similar direction finding measurements of continuum radiation at a lower frequency of 31.1 kHz show an even larger fraction of anomalous cases with the radiation also appearing to come from the general region of the bow shock and/or magnetosheath.

In considering possible origins for this anomalous radiation two possible explanations have been considered. First, the radiation

may be generated in the bow shock and/or magnetosheath and therefore not related to the magnetospheric continuum radiation. Second, it is possible that the "anomalous" direction finding results may be the results of scattering, reflection, or partial obscuration of the magnetospheric continuum by the magnetosheath at times when the solar wind and magnetosheath plasma frequency are unusually high, near 56.2 kHz. The present indications are that the anomalous radiation is actually generated near the bow shock and is not associated with the non-thermal continuum from the magnetosphere. Although usually very weak the frequency spectrum of the anomalous radiation sometimes exhibits a distinct enhancement in a single frequency channel, suggestive of a line emission rather than a continuum. Since 56.2 kHz is approximately twice the solar wind plasma frequency the most likely possibility is that this radiation is produced at twice the solar wind plasma frequency by non-linear interactions with electrostatic electron plasma oscillations, as suggested by Ginzburg and Zheleznyakov [1958] for type III radio noise bursts. The source location of the anomalous 56.2 kHz radiation, near the bow shock on the morning side of the magnetosphere, is consistent with the favored region for electron plasma oscillations excited by energetic electrons streaming into the solar wind from the bow shock [Scarf et al., 1971; Fredricks et al., 1971]. Electromagnetic emissions of this type, at the second harmonic of the plasma frequency, have been previously observed near the bow shock region by Dunckel [1973].

VI. DISCUSSION

We have shown that a weak non-thermal continuum is produced by the earth's magnetosphere extending over a very broad range of frequencies, from as low as 500 Hz in the low density regions of the magnetotail to greater than 100 kHz. The intensity of this continuum decreases rapidly with increasing frequency and is usually not detectable, above the galactic noise background, at frequencies greater than about 100 kHz. At frequencies below the solar wind plasma frequency, which is typically about 20 kHz, the continuum radiation is trapped within the magnetospheric cavity and cannot escape. The "Q" of the cavity is evidently quite low because only a small, factor of two, increase in intensity is observed as the frequency changes from the free escape to the trapped regimes. Direction finding measurements indicate a distinct directionality to the trapped continuum radiation in the distant magnetotail, with the ray paths aligned roughly along the earth-sun line, suggesting that the dayside magnetopause boundary acts as a giant parabolic reflector directing radiation from near the earth into the downstream tail region.

The spatial distribution of intensity for both the trapped and freely escaping continuum radiation and the direction finding measurements for the escaping component all indicate that the radiation is generated in a broad region located outside of the plasmapause at

radial distances from 4.0 R_e to 8.0 R_e and extending through the local morning and early afternoon from about 4.0 hours to 14.0 hours local time. In contrast to auroral kilometric radiation, which is generated in the high latitude auroral zone regions, the continuum radiation appears to be generated at low to moderate latitudes, including the magnetic equator. The continuum radiation is often observed immediately beyond the propagation cutoff at $f \simeq f_p$ near the magnetic equator with no evidence of an equatorial shadow zone such as is observed for auroral kilometric radiation [Gurnett, 1974].

Frankel [1973] has proposed that the non-thermal continuum radiation from the earth's magnetosphere is produced by gyro-synchrotron radiation from energetic electrons in the outer radiation zone. In many respects the results of this study are in reasonably good agreement with Frankel's calculations. The frequency spectrum of the escaping radiation, the radial location of the source, and the power flux (within a factor of 5 to 15, depending on the model) are all in tolerable agreement with the gyro-synchrotron radiation model. No calculations are available for comparison with the trapped continuum radiation. However, some problems are presented by these new data. As shown by the intensity measurements in Figures 9 and 14 a pronounced local time assymmetry is evident in the source intensity, with a distinct maximum in the range from 4.0 hours to 14.0 hours local time. Since most of the energy radiated by the gyro-synchrotron mechanism comes from electrons with energies from 100 keV to 500 keV it is hard to see how this local time assymmetry can occur for these very high

energies. The dawn to dusk electric field within the magnetosphere does tend to increase the electron energies in the local morning region by on the order of 10 keV, however this energy change is essentially trivial for the electrons contributing to the gyro-synchrotron radiation. It is possible that the evening bulge in the plasmasphere may be able to account for part of this assymmetry, although it seems unlikely that the bulge can account for the large asymmetry actually observed.

The radial intensity profiles of the continuum radiation, such as shown in Figure 13, also do not agree with what would be expected for the gyro-synchrotron mechanism. For the synchrotron mechanism one would expect the intensity to gradually increase with increasing radial distance beyond the plasmapause with the maximum intensity occurring near the center of the emitting region. Instead the maximum intensity sometimes occurs almost immediately after crossing the plasmapause (as in the top two panels of Figure 13), directly in the region where the electrostatic noise bands at $f \simeq f_p$ are observed. Cases of this type strongly suggest that the electrostatic noise bands at $f \simeq f_p$ are in some way closely associated with the generation of the continuum radiation.

Recently Shaw and Gurnett [1975] completed a study of the electrostatic noise bands of the type illustrated in Figure 13. These noise bands are shown to consist of high order $(n + 1/2)f_g$ harmonics of the electron gyrofrequency which become strongly enhanced at frequencies near the local plasma frequency. These noise bands are

essentially a permanent feature of the magnetosphere and, interestingly, have maximum intensity in the same local time range in which the continuum radiation appears to be generated. Since the power radiated by the incoherent gyro-synchrotron mechanism is about a factor of 5 to 15 too small [see Frankel, 1974] it may be that electrostatic waves of this type play an important role in the generation of electromagnetic radiation at frequencies above the local plasma frequency.

ACKNOWLEDGMENTS

I wish to extend my thanks to Dr. M. Montgomery who provided the solar wind plasma density data and to Mr. M. Baumback and Mr. R. Anderson for their assistance in the data analysis.

This work was supported in part by the National Aeronautics and Space Administration under contracts NAS5-11074 and NAS5-11431 and Grants NGL-16-001-043 and NGL-16-001-002 and by the Office of Naval Research under Grant N00014-68-A-0196-0009.

REFERENCES

Brown, L. W., The galactic radio spectrum between 130 kHz and 2600 kHz, Astrophys. J., 180, 359, 1973.

Carpenter, D. L., Whistler evidence of the dynamic behavior of the dusk side bulge in the plasmasphere, J. Geophys. Res., 75, 3837, 1970.

Dunckel, N., Plasma oscillations in the solar wind, Abstract, EOS Trans. AGU, 54, 442, 1973.

Frankel, M. S., LF radio noise from the Earth's magnetosphere, Radio Science, 8, 991, 1973.

Fredricks, R. W., F. L. Scarf, and L. A. Frank, Non-thermal electrons and high frequency waves in the upstream solar wind: Parts 2, Analysis and interpretation, J. Geophys. Res., 76, 6691, 1971.

Ginzburg, V. L. and V. V. Zheleznyakov, On the possible mechanisms of sporadic radio emission (Radiation in an isotropic plasma), Soviet Astron., 2, 653, 1958.

Gurnett, D. A., The earth as a radio source: Terrestrial kilometric radiation, J. Geophys. Res., 79, 4227, 1974.

Gurnett, D. A. and R. R. Shaw, Electromagnetic radiation trapped in the magnetosphere above the plasma frequency, J. Geophys. Res., 78, 8136, 1973.

Kaiser, M. L. and R. G. Stone, Observations of the earth at low frequencies, paper 1-2, 1974 URSI meeting, October 14-17, Boulder, Colorado, 1974.

Kurth, W. S., M. M. Baumback, and D. A. Gurnett, Direction finding measurements of auroral kilometric radiation, J. Geophys. Res., (submitted for publication), 1975.

Scarf, F. L., R. W. Fredricks, L. A. Frank, and M. Neugebauer, Nonthermal electrons and high frequency waves in the upstream solar wind: Part 1, Observations, J. Geophys. Res., 76, 5162, 1971.

Shaw, R. R. and D. A. Gurnett, Electrostatic noise bands associated with the electron gyrofrequency and plasma frequency in the outer magnetosphere, J. Geophys. Res., (submitted for publication), 1975.

FIGURE CAPTIONS

Figure 1 The electric field intensities observed at 16 frequencies for a 24 hour period of IMP-8 data in the solar wind. The amplitude range for each frequency represents a dynamic range of 100 db. During this day only one interval, from about 1005 UT to 1115 UT, occurs in which the intensity of the auroral kilometric radiation drops to a level sufficiently low to determine the complete spectrum of the non-thermal continuum.

Figure 2 A selected continuum spectrum in the distant magnetotail. Note that the spectrum of the continuum radiation extends to considerably lower frequencies in the magnetotail than in the solar wind.

Figure 3 Selected spectrums of the non-thermal continuum at various local times. The abrupt cutoff in the solar wind spectrums at about 20 kHz occurs at the local solar wind plasma frequency. Note that the spectrum in the magnetotail extends to frequencies well below the cutoff observed in the solar wind.

Figure 4 The spectrums of the galactic background, the auroral kilometric radiation, and the non-thermal continuum radiation as would be observed by a satellite about 30 R_e from the earth. The trapped continuum radiation can only be detected within the magnetospheric cavity.

Figure 5 Direction finding measurements showing the shift in the null direction, δ, and the modulation factor, m, of the continuum radiation at the solar wind plasma frequency. These measurements were made in the magnetotail at a local time of 22.5 hours.

Figure 6 Direction finding measurements in the magnetotail similar to Figure 5 except at a local time of 1.8 hours. In both cases the null direction of the trapped continuum radiation shifts toward the sun at frequencies below the solar wind plasma frequency.

Figure 7 A series of measurements in the magnetotail showing that the null direction of the trapped continuum radiation is consistently aligned along the satellite-sun line.

Figure 8 A qualitative indication of the ray paths from a source near the earth at frequencies above and below the plasma frequency in the magnetosheath. When $f < f_p$ (magnetosheath)

reflections at the magnetopause tend to align the average ray path direction in the distant magnetotail along the earth-sun line.

Figure 9 The intensity distribution of the trapped continuum radiation at 16.5 kHz. A distinct maximum in the radiation intensity occurs in the local time range from 4.0 hours to 14.0 hours at radial distances from about 5.01 R_e to 7.94 R_e.

Figure 10 The distribution of transverse source positions obtained for 82 direction finding measurements of the escaping continuum radiation at various local times around the earth.

Figure 11 Ray paths obtained from direction finding measurements of the escaping continuum radiation at various local times. Most of the radiation appears to be coming from the local morning and early afternoon at a radial distance of about 2 R_e to 3 R_e from the center of the earth.

Figure 12 The modulation factor of the escaping continuum radiation corrected for errors introduced by the receiver noise level and the latitudinal location of the source. The angular size of the source can be roughly estimated from the modulation factor.

Figure 13 The radial variation of intensity for three cases in which the intensity of the continuum radiation is well above the noise level of the IMP-6 experiment. In some cases the continuum radiation appears to be closely associated with the electrostatic noise bands at $f \simeq f_p$ located near the plasmapause.

Figure 14 The distribution of intensity of the escaping continuum radiation at 56.2 kHz. Again a distinct maximum is evident in the local time range from 4.0 hours to 14.0 hours just beyond the plasmapause.

Figure 15 A qualitative sketch of the source region of the continuum radiation indicated by the direction finding measurements in Figure 11 and the intensity distributions in Figures 9 and 14.

Figure 16 The ray path directions for the anomalous direction finding measurements at 56.2 kHz. Note that many of the ray paths appear to intersect near the bow shock on the morning side of the earth.

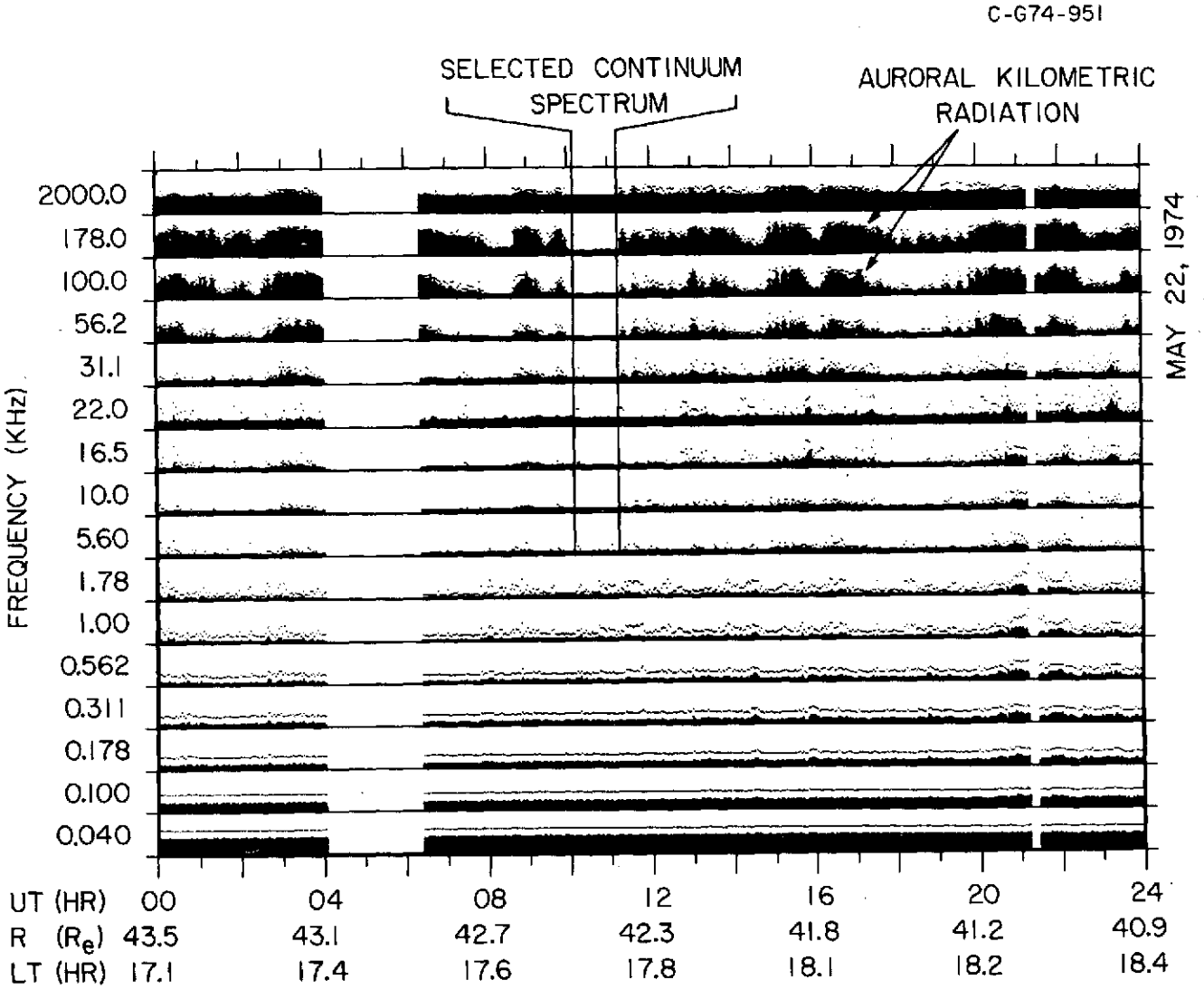
C-G74-951
SELECTED CONTINUUM SPECTRUM
AURORAL KILOMETRIC RADIATION
MAY 22, 1974
FREQUENCY (KHz)
2000.0
178.0
100.0
56.2
31.1
22.0
16.5
10.0
5.60
1.78
1.00
0.562
0.311
0.178
0.100
0.040
UT (HR) 00 04 08 12 16 20 24
R (Re) 43.5 43.1 42.7 42.3 41.8 41.2 40.9
LT (HR) 17.1 17.4 17.6 17.8 18.1 18.2 18.4

Figure 1

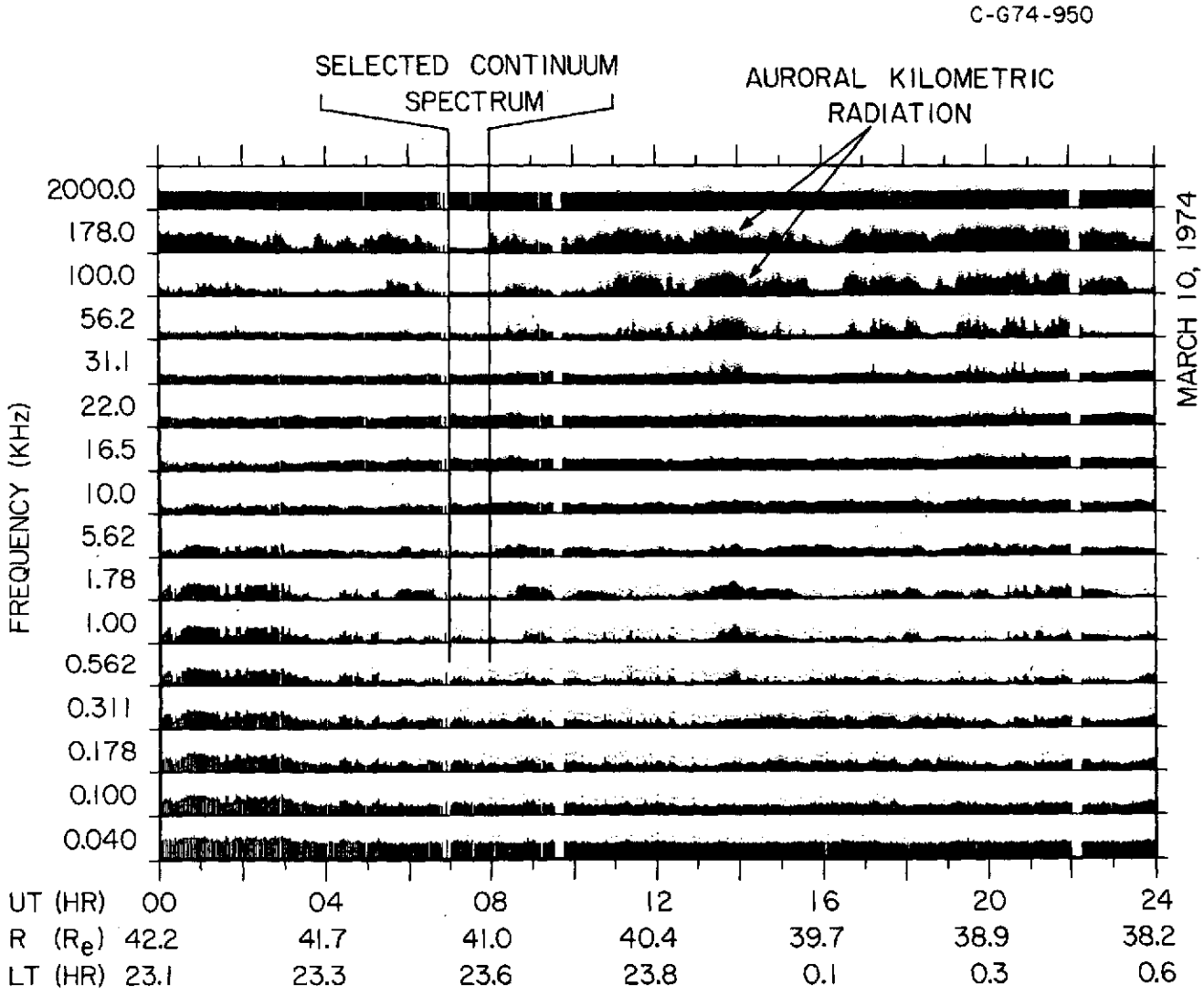
C-G74-950
SELECTED CONTINUUM SPECTRUM
AURORAL KILOMETRIC RADIATION
FREQUENCY (KHz)
2000.0
178.0
100.0
56.2
31.1
22.0
16.5
10.0
5.62
1.78
1.00
0.562
0.311
0.178
0.100
0.040
MARCH 10, 1974
UT (HR) 00 04 08 12 16 20 24
R (Re) 42.2 41.7 41.0 40.4 39.7 38.9 38.2
LT (HR) 23.1 23.3 23.6 23.8 0.1 0.3 0.6

Figure 2

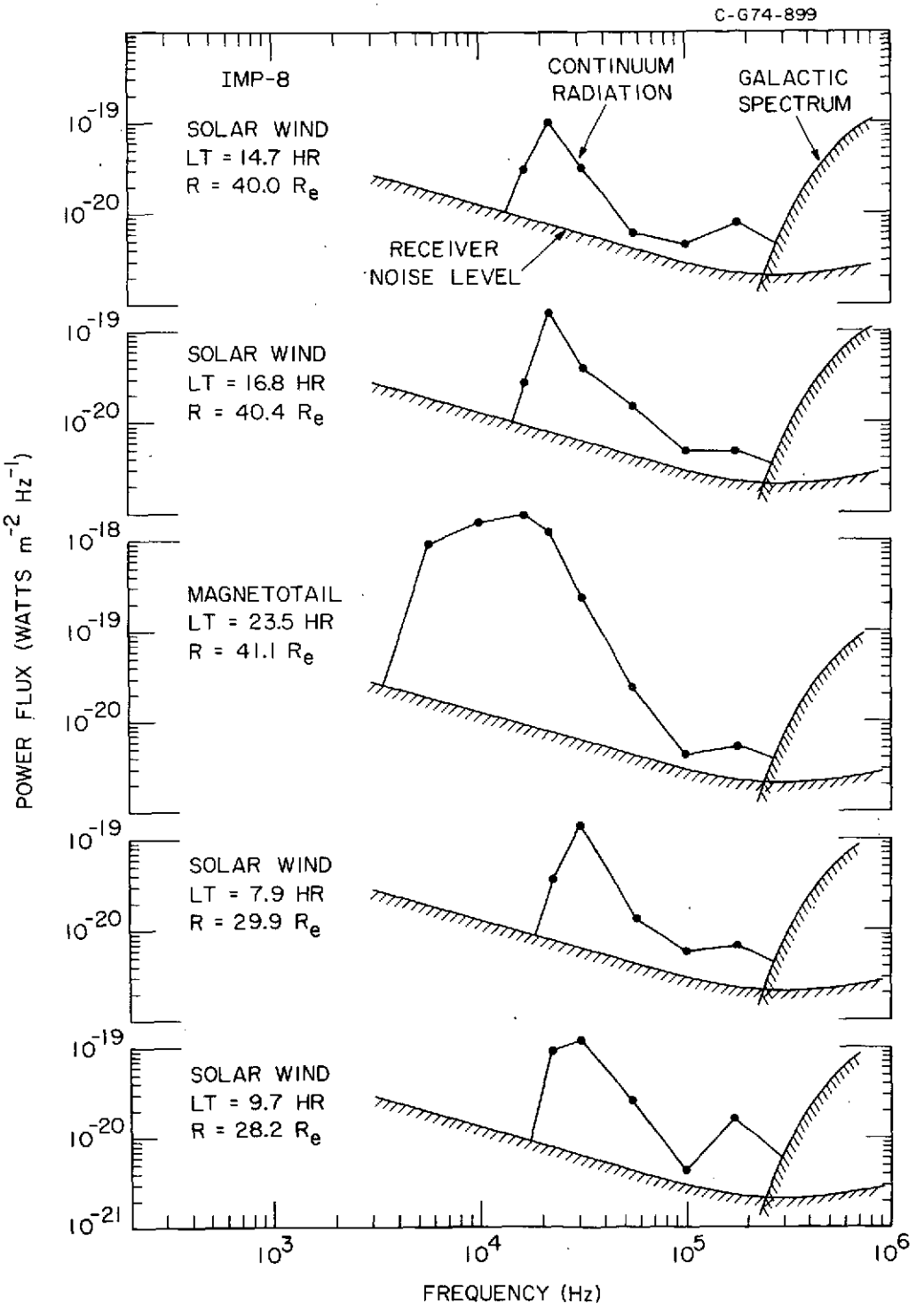
C-G74-899
IMP-8
SOLAR WIND
LT = 14.7 HR
R = 40.0 Re
CONTINUUM RADIATION
GALACTIC SPECTRUM
RECEIVER NOISE LEVEL
SOLAR WIND
LT = 16.8 HR
R = 40.4 Re
MAGNETOTAIL
LT = 23.5 HR
R = 41.1 Re
SOLAR WIND
LT = 7.9 HR
R = 29.9 Re
SOLAR WIND
LT = 9.7 HR
R = 28.2 Re
POWER FLUX (WATTS m-2 Hz-1)
FREQUENCY (Hz)

Figure 3

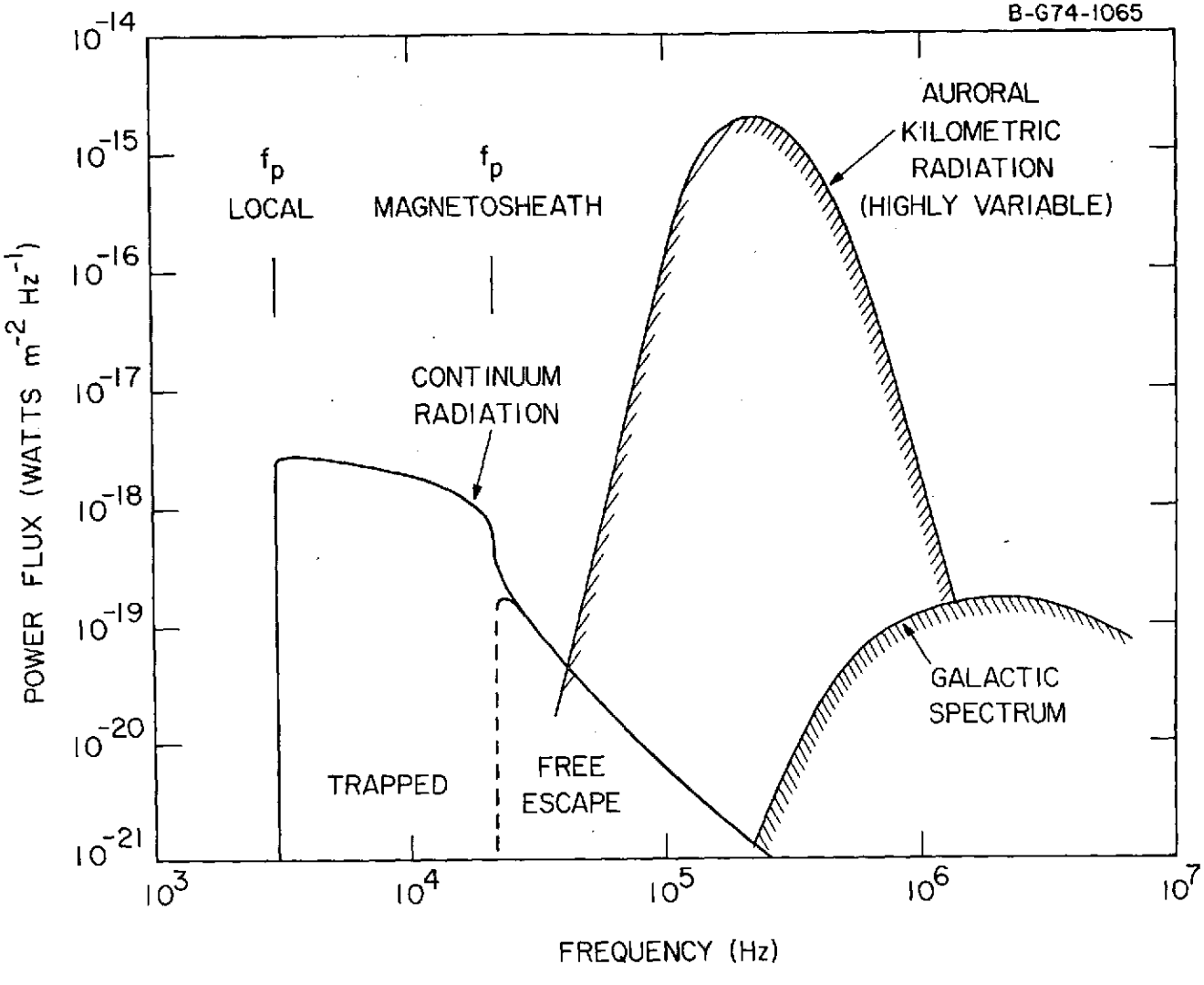
B-G74-1065
AURORAL
KILOMETRIC
RADIATION
(HIGHLY VARIABLE)
f_p
LOCAL
f_p
MAGNETOSHEATH
CONTINUUM
RADIATION
GALACTIC
SPECTRUM
TRAPPED
FREE
ESCAPE
POWER FLUX (WATTS m^{-2} Hz^{-1})
FREQUENCY (Hz)
10^{-14}
10^{-15}
10^{-16}
10^{-17}
10^{-18}
10^{-19}
10^{-20}
10^{-21}
10^{3}
10^{4}
10^{5}
10^{6}
10^{7}

Figure 4

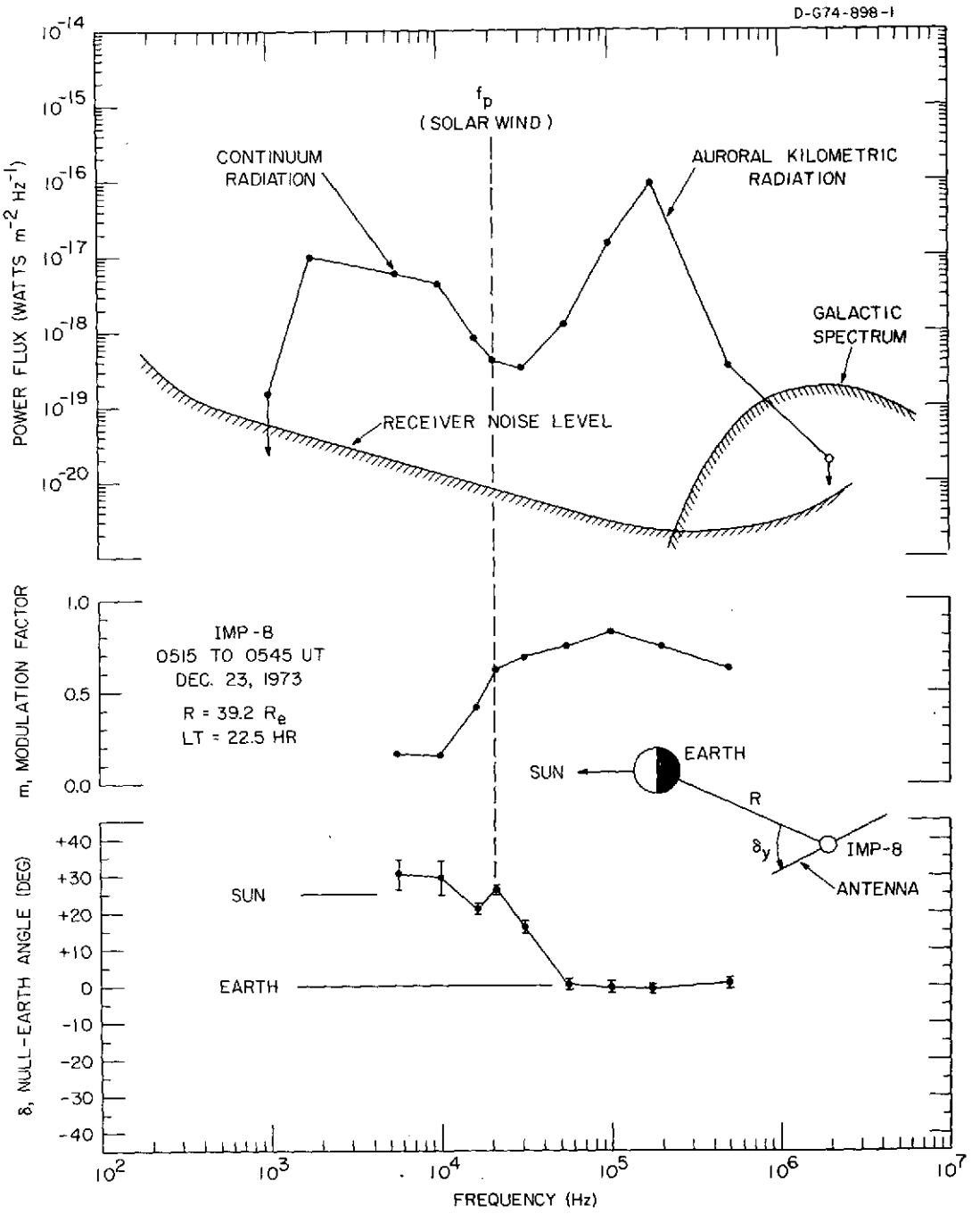
D-G74-898-I
POWER FLUX (WATTS m⁻² Hz⁻¹)
10⁻¹⁴
10⁻¹⁵
10⁻¹⁶
10⁻¹⁷
10⁻¹⁸
10⁻¹⁹
10⁻²⁰
fp
(SOLAR WIND)
CONTINUUM RADIATION
AURORAL KILOMETRIC RADIATION
GALACTIC SPECTRUM
RECEIVER NOISE LEVEL
IMP-8
0515 TO 0545 UT
DEC. 23, 1973
R = 39.2 Re
LT = 22.5 HR
m, MODULATION FACTOR
1.0
0.5
0.0
SUN
EARTH
R
δy
IMP-8
ANTENNA
δ, NULL-EARTH ANGLE (DEG)
+40
+30
+20
+10
0
-10
-20
-30
-40
SUN
EARTH
10²
10³
10⁴
10⁵
10⁶
10⁷
FREQUENCY (Hz)

Figure 5

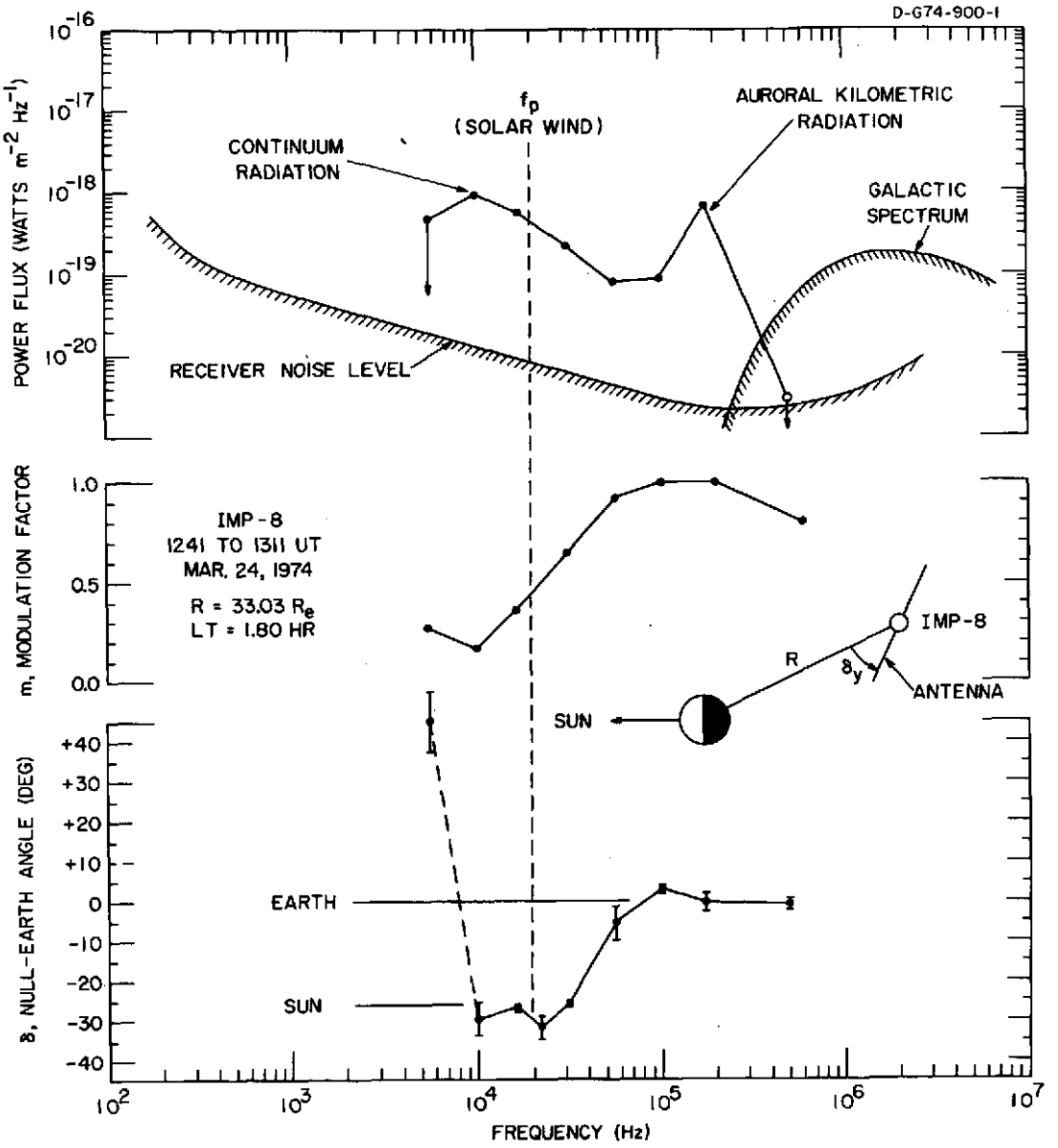
D-G74-900-1
POWER FLUX (WATTS m^{-2} Hz^{-1})
10^{-16}
10^{-17}
10^{-18}
10^{-19}
10^{-20}
f_p
(SOLAR WIND)
CONTINUUM
RADIATION
AURORAL KILOMETRIC
RADIATION
GALACTIC
SPECTRUM
RECEIVER NOISE LEVEL
m, MODULATION FACTOR
1.0
0.5
0.0
IMP-8
1241 TO 1311 UT
MAR. 24, 1974
R = 33.03 R_e
LT = 1.80 HR
IMP-8
R
δ_y
ANTENNA
SUN
δ, NULL-EARTH ANGLE (DEG)
+40
+30
+20
+10
0
-10
-20
-30
-40
EARTH
SUN
10^2
10^3
10^4
10^5
10^6
10^7
FREQUENCY (Hz)

Figure 6

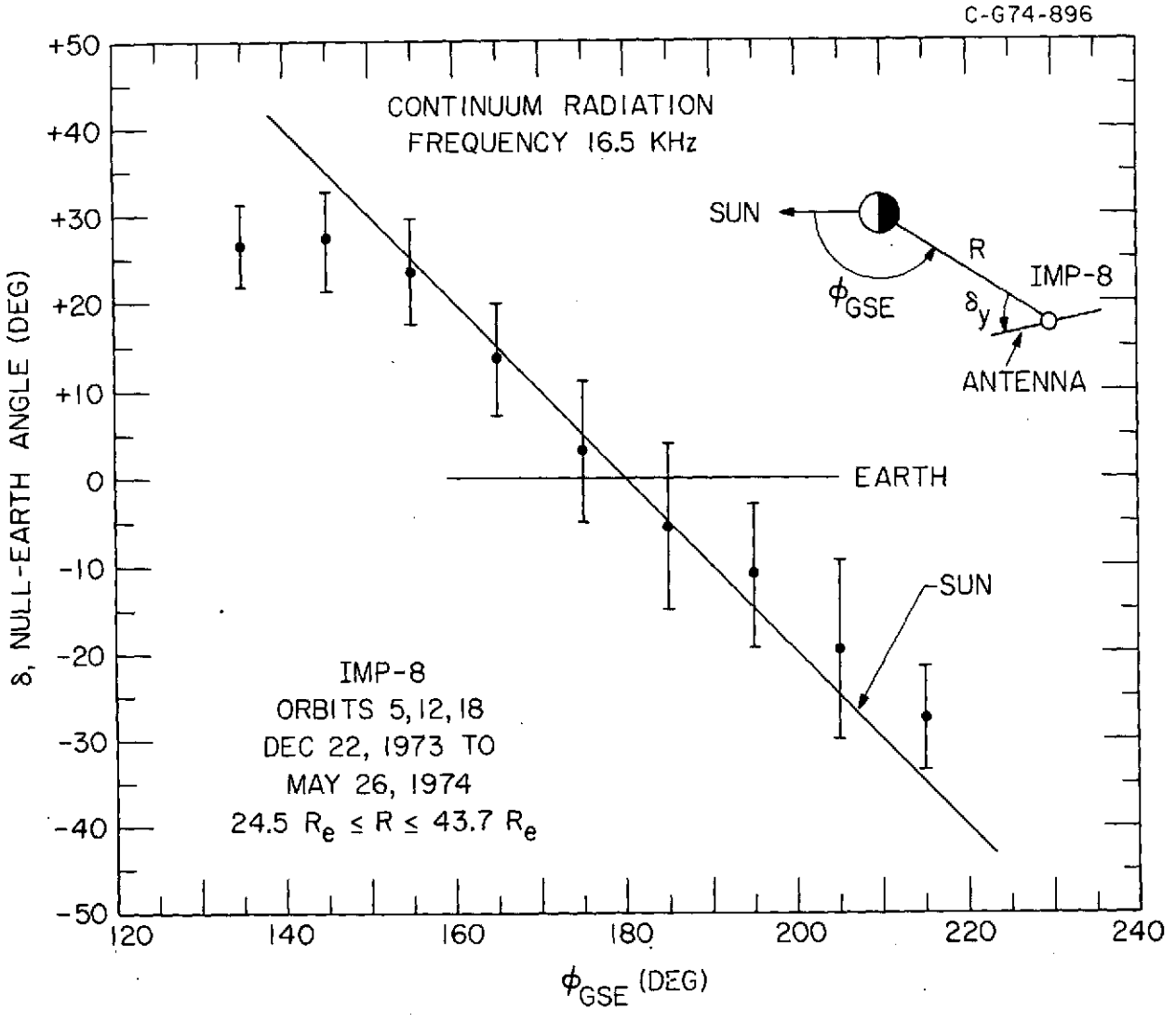
C-G74-896
CONTINUUM RADIATION
FREQUENCY 16.5 KHz
SUN
R
IMP-8
ϕ_{GSE}
δ_y
ANTENNA
EARTH
SUN
IMP-8
ORBITS 5, 12, 18
DEC 22, 1973 TO
MAY 26, 1974
24.5 $R_e \leq R \leq$ 43.7 R_e
δ, NULL-EARTH ANGLE (DEG)
+50
+40
+30
+20
+10
0
-10
-20
-30
-40
-50
120
140
160
180
200
220
240
ϕ_{GSE} (DEG)

Figure 7

B-G74-801-I

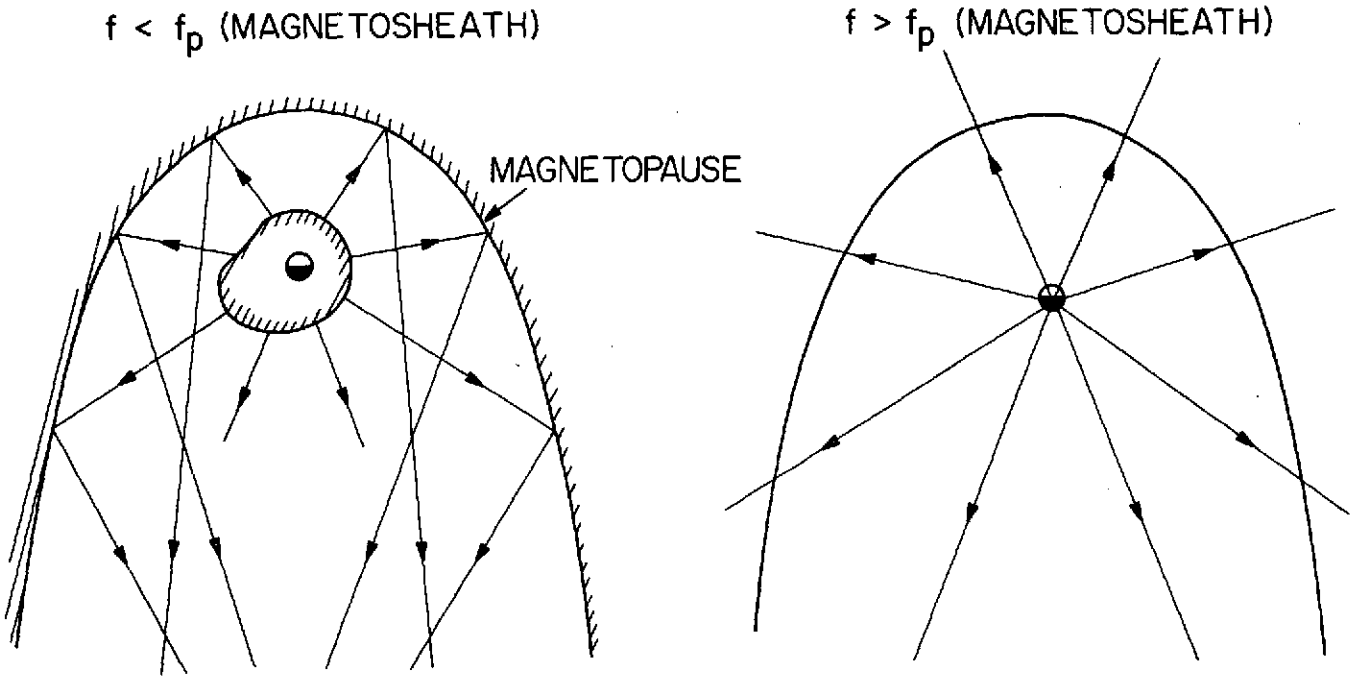

Figure 8

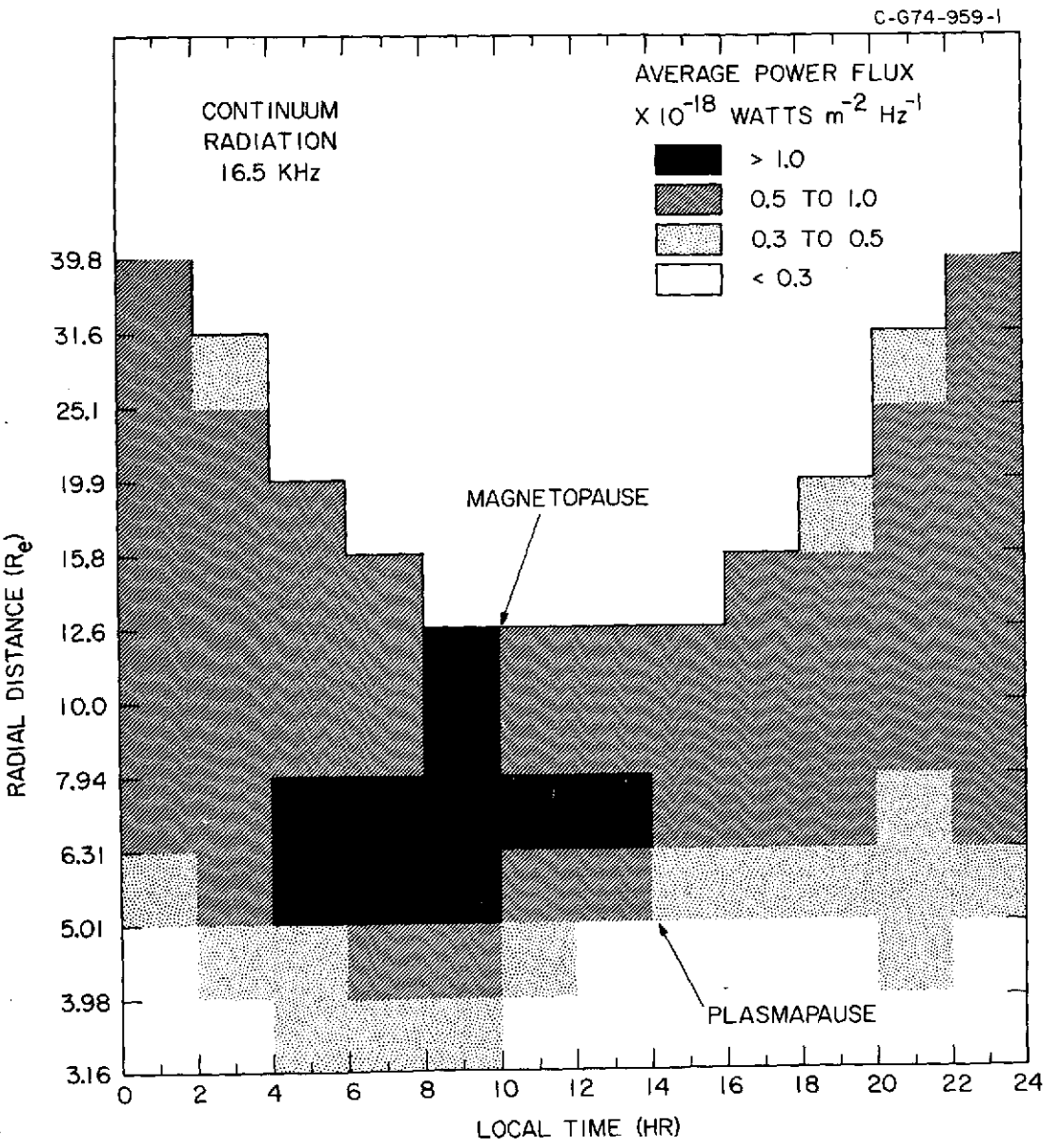
C-G74-959-1
CONTINUUM
RADIATION
16.5 KHz
AVERAGE POWER FLUX
X 10^-18 WATTS m^-2 Hz^-1
> 1.0
0.5 TO 1.0
0.3 TO 0.5
< 0.3
MAGNETOPAUSE
PLASMAPAUSE
RADIAL DISTANCE (Re)
39.8
31.6
25.1
19.9
15.8
12.6
10.0
7.94
6.31
5.01
3.98
3.16
0
2
4
6
8
10
12
14
16
18
20
22
24
LOCAL TIME (HR)

Figure 9

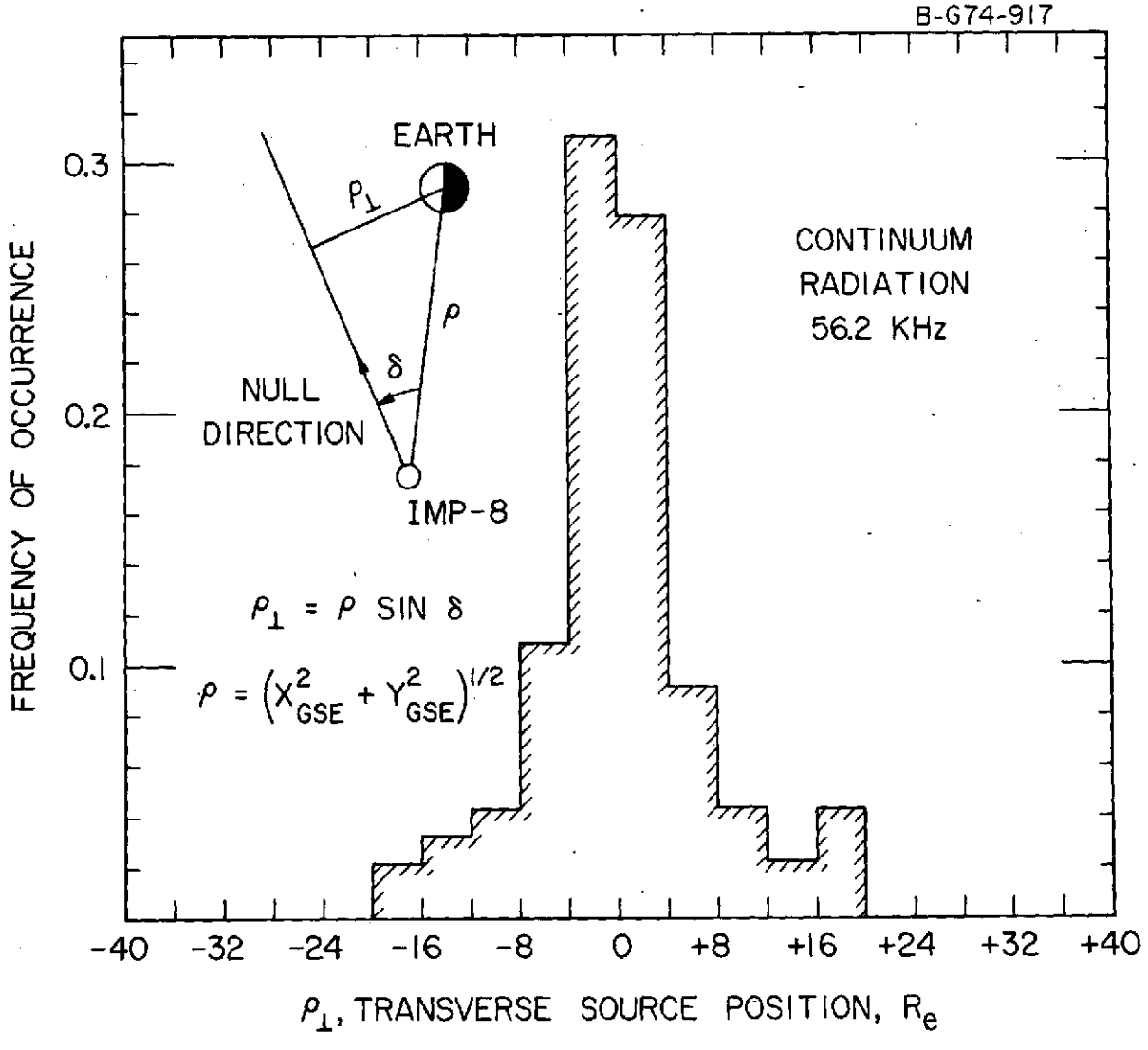
B-G74-917
EARTH
$\rho_\perp$
ρ
δ
NULL
DIRECTION
IMP-8
CONTINUUM
RADIATION
56.2 KHz
$\rho_\perp = \rho \sin \delta$
$\rho = \left(X^2_{GSE} + Y^2_{GSE}\right)^{1/2}$
FREQUENCY OF OCCURRENCE
0.3
0.2
0.1
-40
-32
-24
-16
-8
0
+8
+16
+24
+32
+40
$\rho_\perp$, TRANSVERSE SOURCE POSITION, R_e

Figure 10

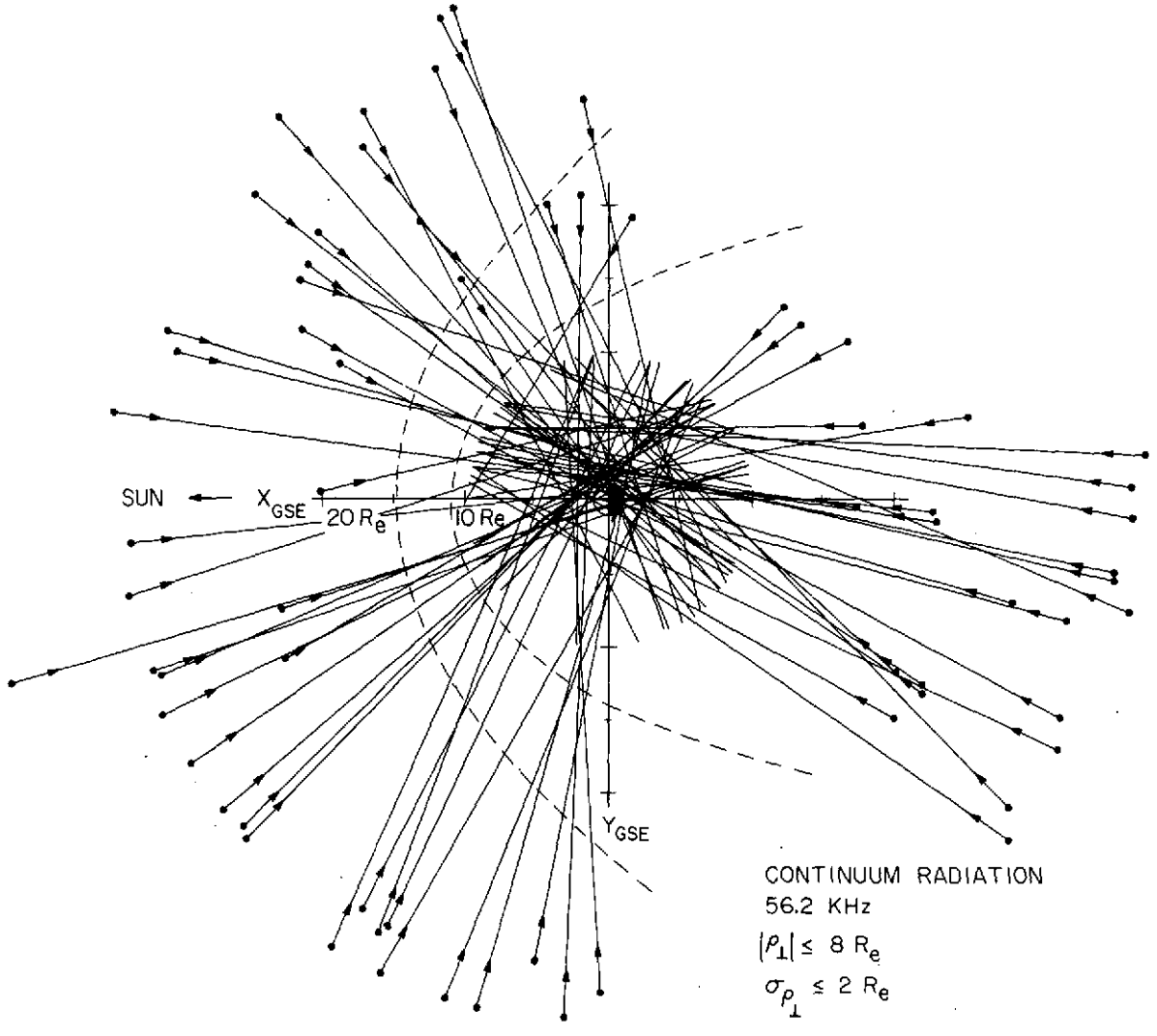
SUN
X_{GSE}
20 R_e
10 Re
Y_{GSE}
CONTINUUM RADIATION
56.2 KHz
$|\rho_\perp| \leq 8\ R_e$
$\sigma_{\rho_\perp} \leq 2\ R_e$

Figure 11

C-G74-952-I

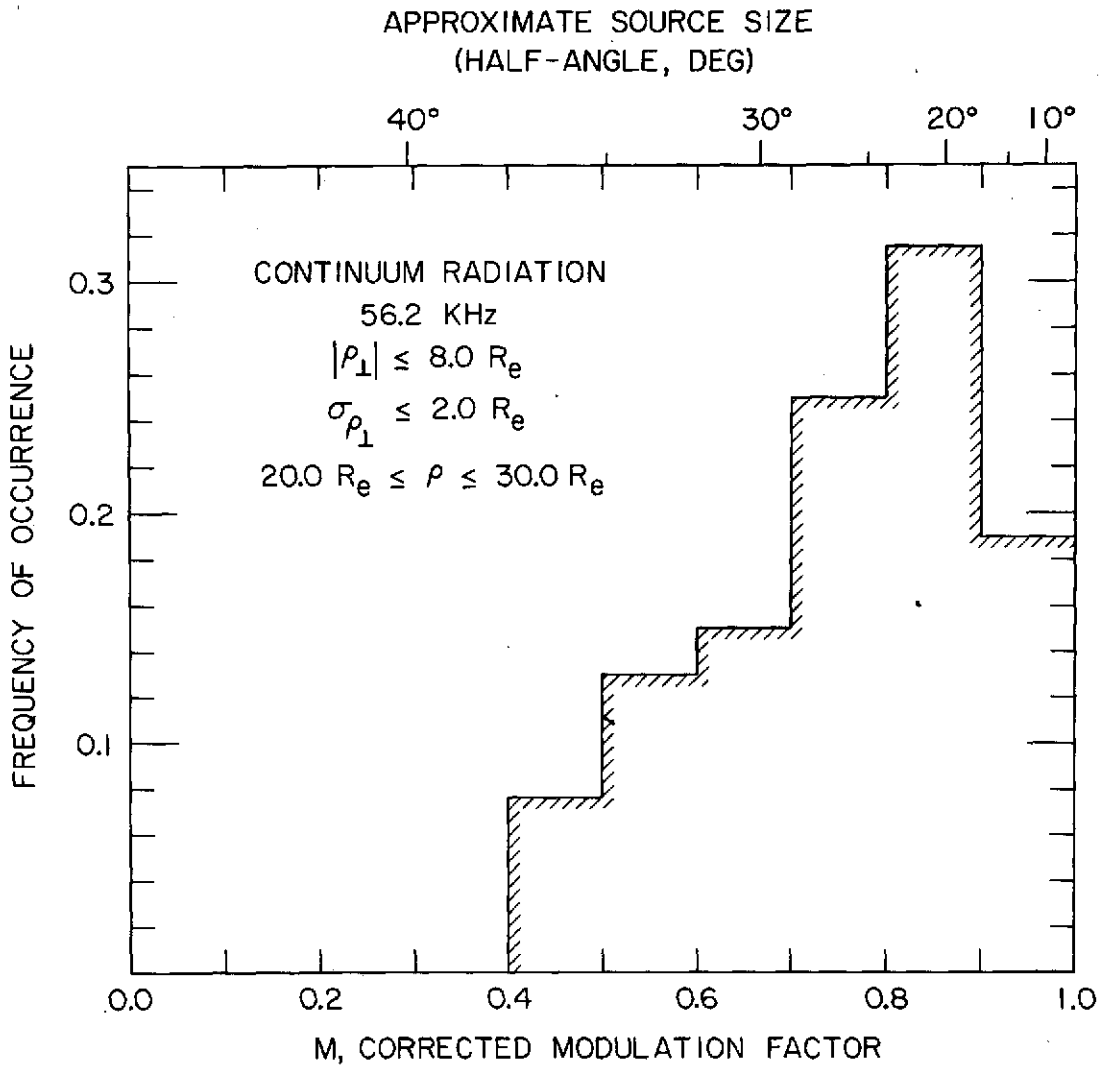

Figure 12

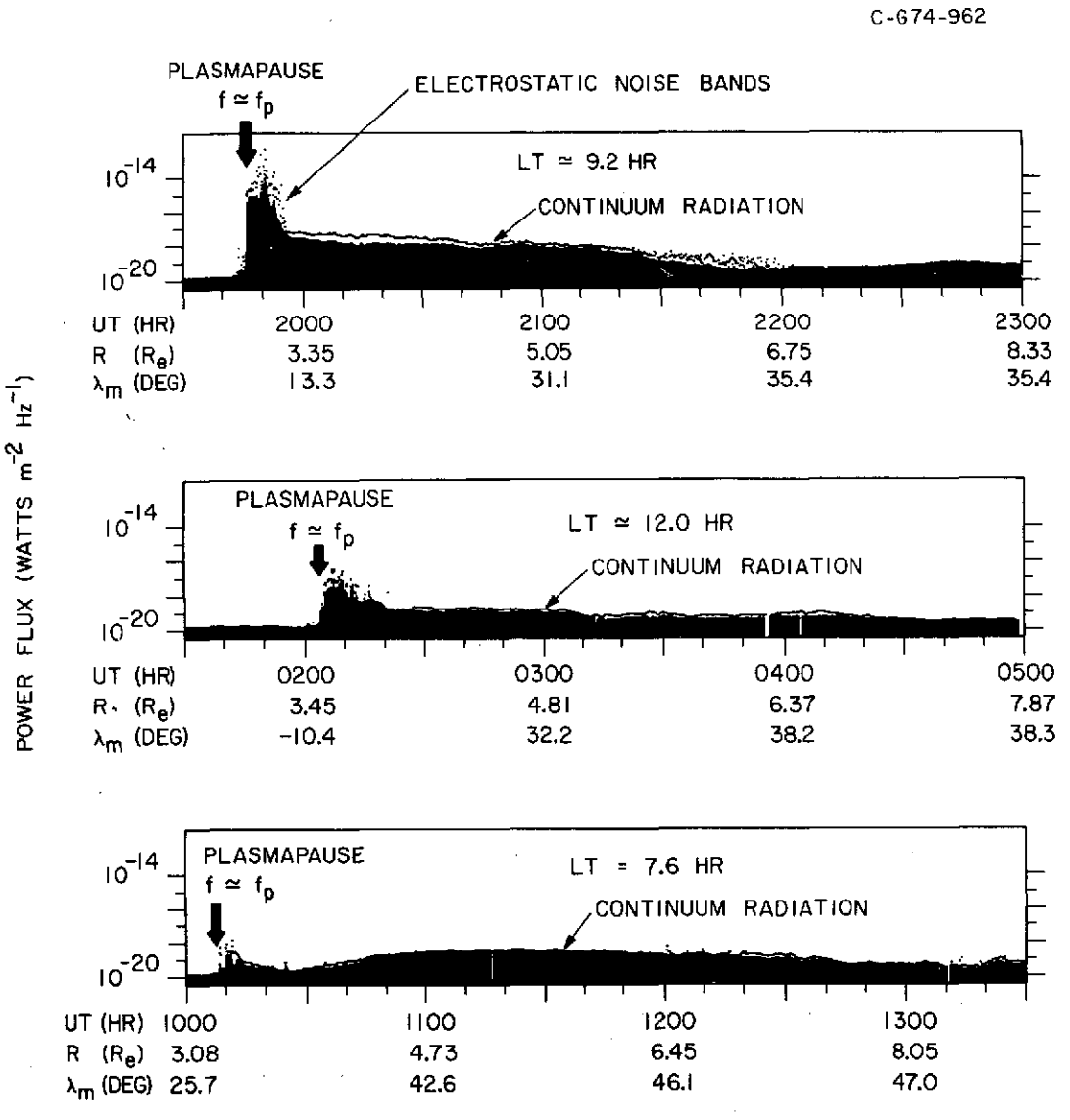
C-G74-962
PLASMAPAUSE
f ≃ fp
ELECTROSTATIC NOISE BANDS
LT ≃ 9.2 HR
CONTINUUM RADIATION
10-14
10-20
UT (HR) 2000 2100 2200 2300
R (Re) 3.35 5.05 6.75 8.33
λm (DEG) 13.3 31.1 35.4 35.4
PLASMAPAUSE
f ≃ fp
LT ≃ 12.0 HR
CONTINUUM RADIATION
UT (HR) 0200 0300 0400 0500
R (Re) 3.45 4.81 6.37 7.87
λm (DEG) -10.4 32.2 38.2 38.3
PLASMAPAUSE
f ≃ fp
LT = 7.6 HR
CONTINUUM RADIATION
UT (HR) 1000 1100 1200 1300
R (Re) 3.08 4.73 6.45 8.05
λm (DEG) 25.7 42.6 46.1 47.0
POWER FLUX (WATTS m-2 Hz-1)

Figure 13

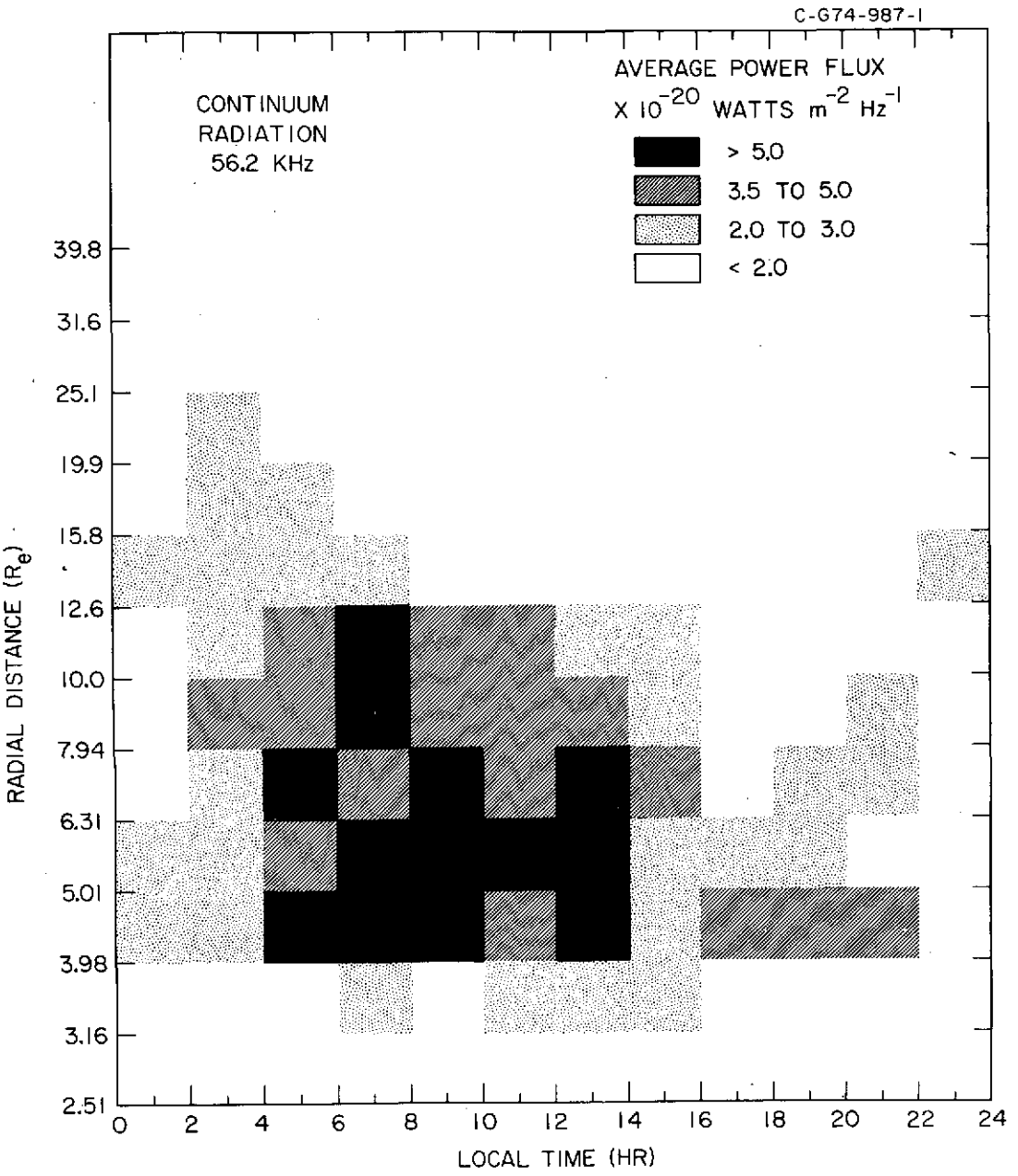
C-G74-987-I
CONTINUUM
RADIATION
56.2 KHz
AVERAGE POWER FLUX
X 10^-20 WATTS m^-2 Hz^-1
> 5.0
3.5 TO 5.0
2.0 TO 3.0
< 2.0
RADIAL DISTANCE (Re)
39.8
31.6
25.1
19.9
15.8
12.6
10.0
7.94
6.31
5.01
3.98
3.16
2.51
0
2
4
6
8
10
12
14
16
18
20
22
24
LOCAL TIME (HR)

Figure 14

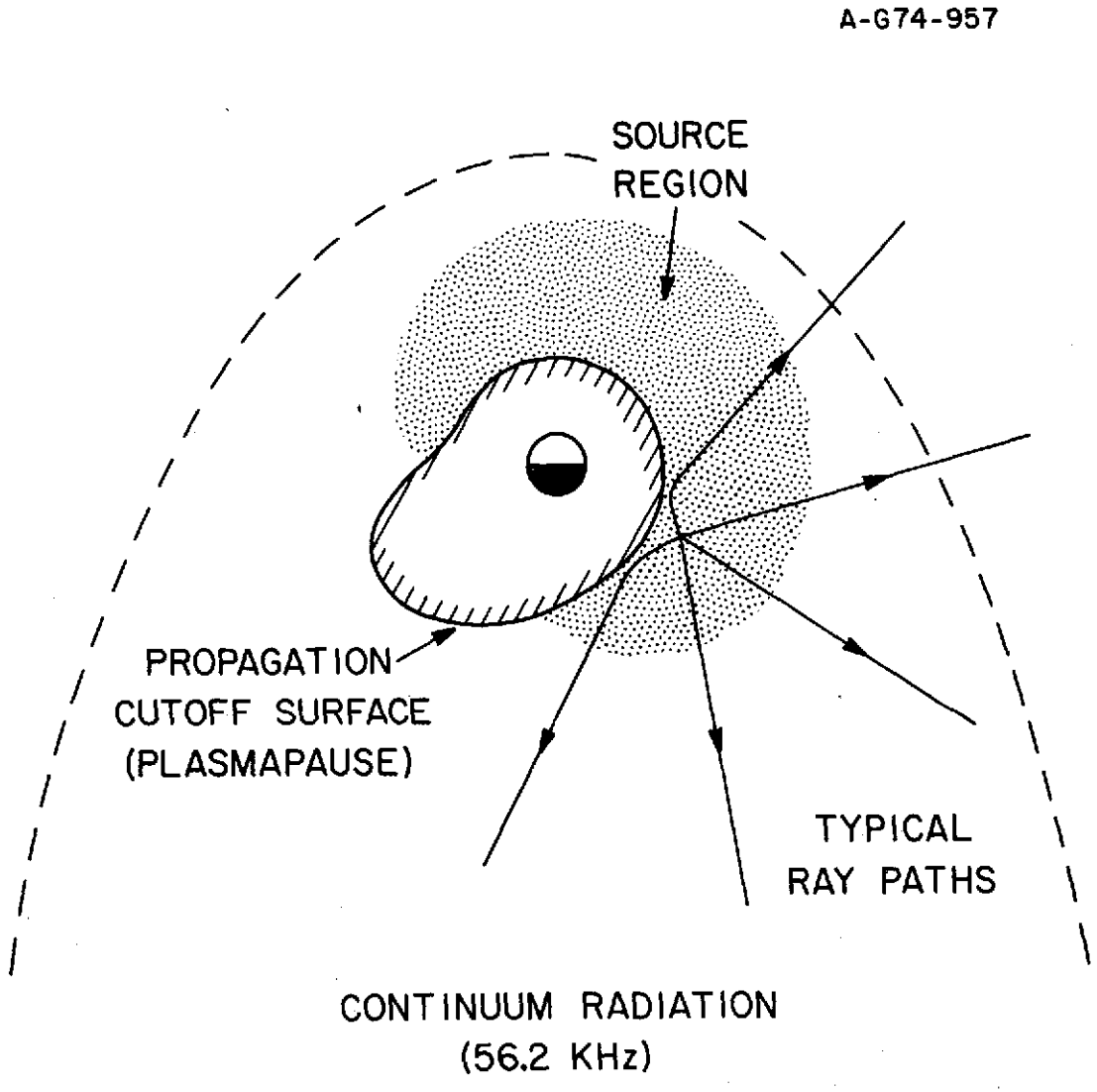
A-G74-957
SOURCE
REGION
PROPAGATION
CUTOFF SURFACE
(PLASMAPAUSE)
TYPICAL
RAY PATHS
CONTINUUM RADIATION
(56.2 KHz)

Figure 15

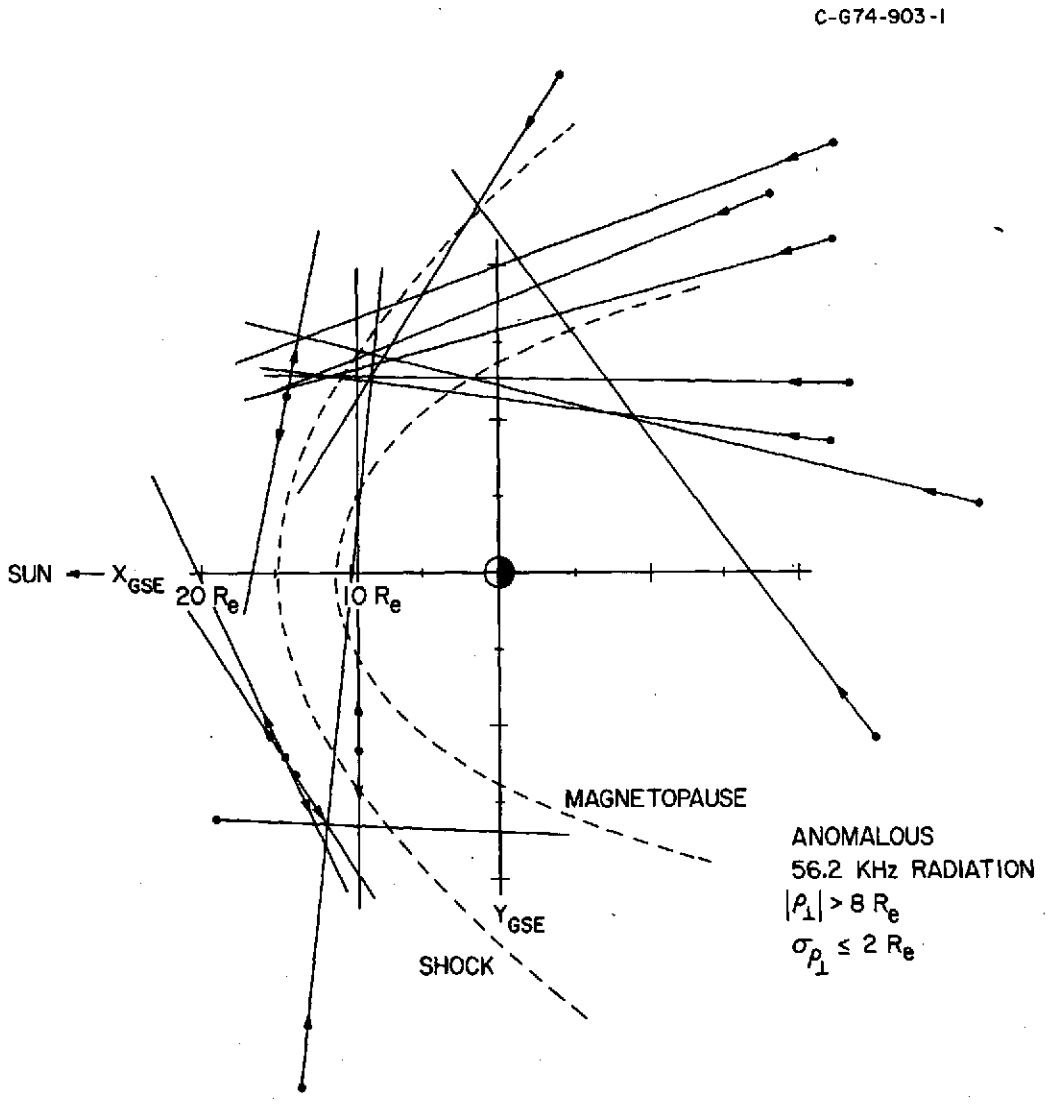
C-G74-903-I
SUN
X_{GSE}
20 R_e
0 R_e
MAGNETOPAUSE
Y_{GSE}
SHOCK
ANOMALOUS
56.2 KHz RADIATION
$|\rho_\perp| > 8\ R_e$
$\sigma_{\rho_\perp} \leq 2\ R_e$

Figure 16